# FUNCTIONAL ANALYSIS OF AN INTEGRATED GTPASE REGULATING THE CELLULAR POOL AND DISTRIBUTION PROFILE OF INTRAFLAGELLAR TRANSPORT PARTICLES IN *CHLAMYDOMONAS REINHARDTII*

A Thesis

by

DAVID ALEJANDRO SILVA

Submitted to the Office of Graduate Studies of
Texas A&M University
in partial fulfillment of the requirements for the degree of

MASTER OF SCIENCE

Approved by:

| | |
|---|---|
| Chair of Committee, | Hongmin Qin |
| Committee Members, | Michael Manson |
| | Hays Rye |
| Head of Department, | U.J. McMahan |

December 2012

Major Subject: Microbiology

ABSTRACT

Cilia and flagella are sensory organelles, found in the majority of eukaryotic organisms that play a vital role in the general physiology, health and early development of humans. Intraflagellar transport (IFT) is tasked with building and maintaining the entire ciliary structure by facilitating the transport of axonemal precursors, trafficking of ciliary membrane proteins and turnover products. Currently, there are no complete models detailing how ciliated organisms regulate the entry and exit of IFT particles, a multi-meric adaptor complex that ferries flagellar proteins. In this thesis, I focus on small Rab-like protein IFT22, an IFT-particle integrated protein with predicted GTPase activity, as a potential regulatory component of IFT particle trafficking in *Chlamydomonas*.

Using an artificial microRNAs strategy, I show that IFT22 regulates the available cellular pool of IFT particles and the distribution profile of the IFT particles between the cytoplasm and the flagellar compartment. Additionally, I demonstrate how the putative constitutive active mutant of IFT22 is able properly localize to the peri-basal body and enter the flagellar compartment using immunofluorescence and immunoblot analysis of flagella extracts. Finally, preliminary RNAi data suggests IFT25 the IFT particle/motor/BBSome assembly downstream of IFT22 regulation, evident from the depletion of kinesin-2 subunit FLA10, IFT-dynein-2 subunit D1bLIC and BBsome component BBS3from whole cell extracts of IFT25 knockdown transformants.

ACKNOWLEDGEMENTS

I would like to thank my committee chair, Dr. Qin, and my committee members, Dr. Rye, and Dr. Manson, for their guidance and support throughout the course of this research. I remembered emailing Dr. Qin during the summer of 2009 asking for chance to work in her lab. Thankfully, because of her, I had to opportunity to attend graduate school here at A&M. Also a special thanks to Dr. Manson for the rounds of beer shared.

Thanks also go to my friends, colleagues and the department faculty for making my time at Texas A&M University a great experience. I also want to extend my gratitude to the Louis Stokes Alliances for Minority Participation Organization, which provided me with enough fellowship money to dedicate myself entirely to research. You cannot imagine how grateful I am to you for your help. To all my Fellows, thank you for all the laughs and good times. BTD VI!

Thanks to my mom and dad for their encouragement and support over the past 25 years. I would not be here if it were not for your love and dedication. To my brother Andrew, I could not have asked for a better friend than you. You kept me sane over the past two years and I am thankful we got to spend more time together before we go start our own families. To my Sigma Lambda Beta brothers, thank you for having my back over the past 6 years. You were my home away from home, and could not ask for a better family to look after Andrew when I leave College Station. And finally, to my best friend and fiancée Crystal, thank you for your love, support and patience during these two years. You are my rock. I am coming home, baby!

TABLE OF CONTENTS

LIST OF FIGURES

# CHAPTER I

# INTRODUCTION*

## BACKGROUND

Cilia and flagella are long, slender structures protruding from the body of ciliated cells and are composed of a microtubule-based core known as the axoneme. The main structural element is an array of microtubule pairs, each pair consisting of a fully enclosed a-subfiber fused to the incomplete b-subfiber with fewer tubulin subunits. In the "9+2" arrangement, nine doublet pairs of subfibers are linked together by nexin proteins that form an enclosed cylinder around a central pair of singlet subfibers. The outer doublet ring and the central pair of microtubules are connected by structures known as radial spokes.[1] The axoneme originates from the basal body, a modified form of the centriole consisting of nine triplet microtubules which anchors the cilia to the plasma membrane. The area between the triplet microtubules of the basal body and doublet pairs of the axoneme is referred to as the transition zone. Proteinaceous extensions from this area called transition fibers serve to mark the enclosure of the flagellar compartment and create a semi-selective barrier from the cytoplasm.
Cilia are categorized into two groups: primary (nonmotile) and motile cilia. Although they have a similar basic structure, the biological functions of primary and motile cilia can be very different. Primary cilia typically lack the central pair of microtubules known

---

as the "9+0" arrangement, and are also missing accessory proteins important for generating the ciliary waveform stroke. This form of cilia is predominately considered as a sensory antenna for the cell due to a highly specialized profile of membrane proteins and an ability to extend into the luminal space of various tissues. Motile cilia/flagella were once considered important only for the locomotion of single-celled organisms. Recent discoveries in ciliary research have demonstrated how essential motile cilia are for various physiological processes, ranging from mucous clearing in the trachea to aiding in establishing proper left-right symmetry in developing organisms.[2] The terms cilia and flagella will be used interchangeably for the remainder of the thesis report because of their structural similarities.

**Intraflagellar Transport**

Intraflagellar transport (IFT) is the bi-directional movement of non-membrane protein particles which travel along the axoneme, between the space of the ciliary membrane and the microtubule core of the flagella. IFT was originally discovered by Kozminksi and colleagues in 1993, using digital interference contrast (DIC) microscopy to visualize the continuous movement of "bulges" beneath the flagella membrane of the bi-flagellated green algae *Chlamydomonas reinhardtii.* [3]. Anterograde movement, towards the ciliary tip or plus end of microtubules, is powered by heterotrimeric kinesin-2 and retrograde movement is driven by cytoplasmic dyein1b. [4-14] A multi-meric protein complex known as the IFT particle is comprised of two large protein sub-complexes, IFT-A and IFT-B, and attaches to IFT motor complex.[5] The axoneme is undergoing

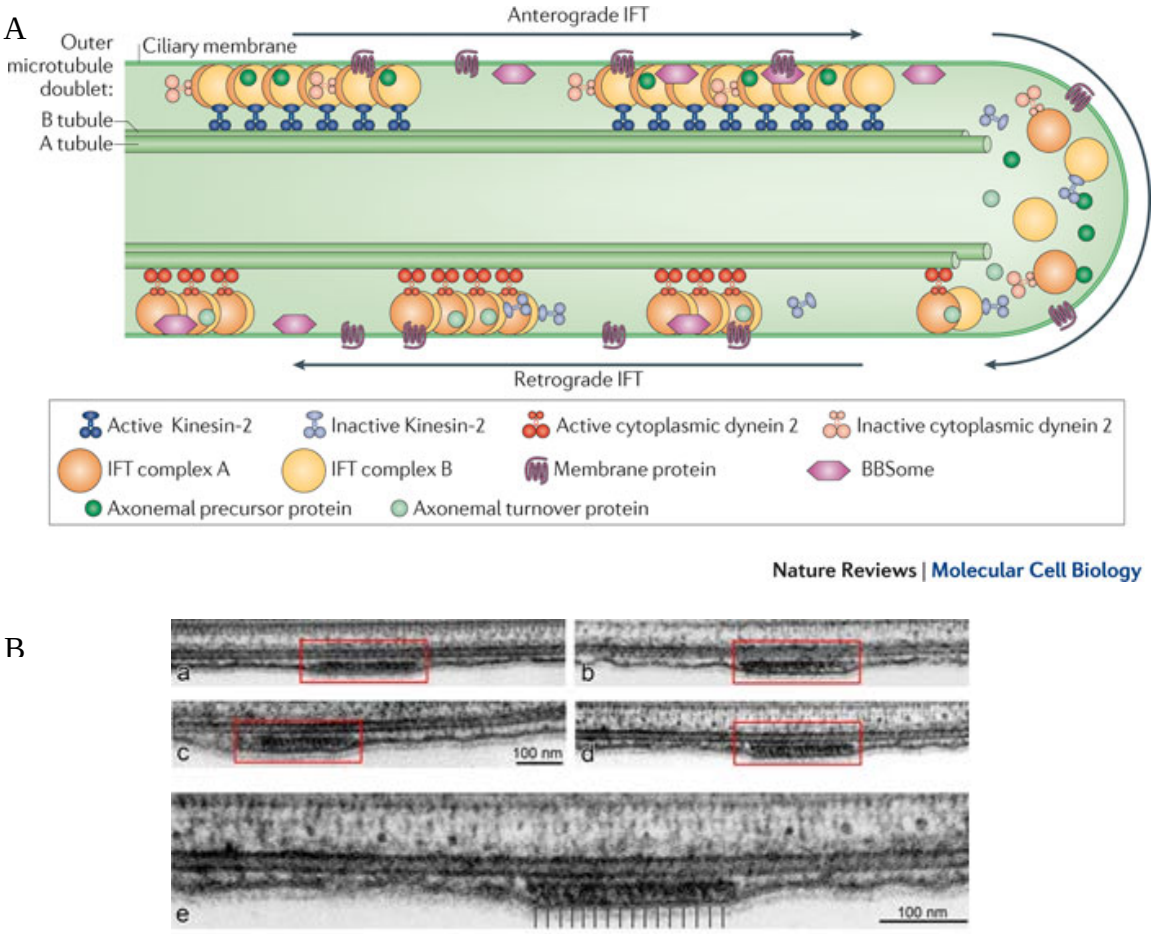


**Figure 1 Intraflagellar transport at a glance.**
A) A simplified version of intraflagellar transport depicts the important components involved in ciliogenesis.[1] Canonical heterotrimeric kinesin-2 powers the anterograde movement of IFT particles and their cargo to the ciliary distal tip. IFT dynein-2 is ferried in the inactivated form until the IFT train reaches the tip; it is at this point that retrograde movement is activated and shuttles turnover products to back into the cell body. B) A TEM cross section capturing IFT trains traveling between the flagellar membrane and the axoneme.[15]

constant protein turnover at its tip, meaning tubulin and other accessory proteins must be constantly replenished to maintain the length of the flagella.[16] The well-conserved IFT motors and particle are tasked with assembling and maintaining the entire cilia structure by serving as an adaptor for the transport of axonemal precursors. Additionally, the IFT assembly ferries in ciliary membrane proteins using a secondary adapter complex known, the BBSome, as an intermediate.[17,18] The following sections will discuss the various members of the IFT machinery and the transition zone as a semi-selective barrier.

**Anterograde Movement: Kinesin-2**

The anterograde IFT motor heterotrimeric kinesin-2 was first isolated in sea-urchin.[19] Homologs are found in a variety of ciliated organisms, including *Tetrahymena*, *Caenorhabditis elegans*, and humans. In *Chlamydomonas*, FLA10 and FLA8 comprise the motor portion of the complex and together they interact with kinesin-associated protein FLA3.[20] First evidence for the role of the kinesin-II in anterograde movement arose from the characterization of a FLA10 temperature sensitive mutant. While incubated at the permissive temperature (22°C), *fla10*$^{ts}$ possess two, full-length flagella. Following a shift to the non-permissive temperature (32°C), FLA10 subunit denatures and IFT proteins are significantly depleted within the first hour.[5] Cessation of IFT results in the dismantling of the axoneme and the entire ciliary structure is eventually retracted into the cell body due to the constant protein turnover. In addition, an isolated

null mutant for the FLA10 subunit produces no flagella[21], further demonstrating the importance of kinesin-2 to ciliogenesis.

These observations, however, are not entirely consistent among all ciliated organisms. Mutations in the kinesin-2 motor subunits of other model organisms do not result in a cilia-less (bald) cell phenotype because of a secondary, homodimeric kinesin known as OSM-3 in *C. elegans* and KIF17 in *Homo sapiens.*[13] Studies investigating the function of OSM-3 conclude that the canonical kinesin-2 motor and OSM-3 work in a concerted effort to build sensory cilia in *C. elegans.*[13] Single null mutants in KLP-11 (FLA8) and KAP-1 (FLA3) in *C. elegans* appear to form intact sensory cilia due to the redundancy of OSM-3 function in ciliogenesis.[22] However, perturbations of OSM-3 results in the loss of the ciliary distal segment comprised of singlet microtubule extensions beyond the doublet axoneme core of *C. elegans* cilia. In these mutants, the heterotrimeric anterograde motor still allows formation of the middle segment.

The transferring of the IFT particle from the canonical kinesin-II to OSM-3 may simply insure the proper and sequential construction of the cilia. However, a previous study observed the speed of OSM-3 actually increases when kinesin-II is compromised[23], suggesting that kinesin-2 may in fact be negatively regulating OSM-3. If so, kinesin-2 would ultimately be involved in determining the re-supply rate of axonemal precursors to the flagella compartment. Defects in retrograde IFT clearly demonstrate the negative impact excess precursors and turnover products have on normal ciliary formation and function. Therefore, the accumulation of axonemal

components caused by an influx of proteins ferried by OSM-3 could also unbalance the natural turnover vs. assembly in favor of creating longer cilia. This exact phenotype has been observed in kinesin-2 mutants. Recently, a null mutant for kinesin-3 KLP-6, a cell-specific kinesin found in *C. elegans* males, demonstrated a slower procession of OSM-3/KAP-1-associated IFT particle within the ciliary compartment.[24] Although it was observed moving independently of the canonical IFT particle/motor complex, KLP-6 function may have a positive influence on ciliary length.

Recently, research has shifted its focus to understanding the process involved in regulating the recruitment of kinesin-2 to the transition zone. Defects in FLA3, a kinesin associated protein, lead to the mislocalization of kinesin-2 and the subsequent production of a bald phenotype in *Chlamydomonas.*[25] Isolation of DYF-11 null mutant, a homolog of human microtubule-interacting protein (MIP)-T3 and IFT54 in *C. elegans*, reveals that this protein may function as an anchoring protein for the priming/loading of the entire IFT motor/particle complex onto the transition zone of cilia.[26] KIF17, an OSM-3 homolog of *C. elegans*, was discovered to be under the regulation of a RAN gradient across the transition zone in human primary cilia. This mechanism was shown to operate much like the RAN gradient active in regulating the trafficking of proteins across the nuclear pore complex.[27] A ciliary localization signal (CLS) at the tail end of KIF17 was shown to contribute to a Ran-GTP inhibited interaction with the nuclear import protein importin-β2. Due to the conserved nature of IFT, it is tempting to

speculate similar CLS signals may exist to regulate the trafficking of other proteins across the transition zone.

**Retrograde Movement: IFT-dynein 2**

IFT-dynein-2, previously known as dynein 1b, powers the retrograde movement of IFT particles.[12] To date, four proteins are confirmed members of the dynein 2 complex: heavy chain DHC1b, light chain LC8, light intermediate chain D1bLIC, and an intermediate chain FAP133. [7-9,14,28-30] *C. elegans* null mutants defective in dynein components undergo normal anterograde movement but accumulate large amounts of IFT proteins and turnover products within the ciliary compartment.[22] Retrograde-defective cilia are severely truncated and contain protein aggregates that appear as noticeable large, electron-dense clots. These results have been observed in *Chlamyomonas*[31], suggesting IFT dynein is responsible for the retrograde movement of the IFT. Anterograde movement remains active in these mutants; however, the characteristic bulbous cilia are present as a result of axonemal turnover outpacing the dysfunctional retrograde IFT. It has become fairly evident that IFT particles do not passively diffuse out of the flagella compartment and turnover products must be actively removed by dynein 2 in order to allow unhindered trafficking of the IFT trains.

The current model for retrograde activation is fragmented at best. IFT-dynein is carried into the compartment in an inactivated form as part of the IFT cargo. Once it reaches the tip, a poorly understood remodeling occurs, ultimately initiating the dynein-powered return of the IFT train back into the cell body.[32,33] During retrograde

movement, the kinesin must be inactivated, though it is unknown whether kinesin-2 is directly removed by the IFT particle as part of the turnover cargo or if it is possibly diffused out. IFT-dynein is historically shown to associate with complex A in *Chlamydomonas*, primarily due to IFT-A temperature sensitive mutants exhibiting similar phenotypes as retrograde mutants. During remodeling at the distal tip, IFT-A likely facilitates the activation of dynein-2 in order to initiate retrograde movement [34], although a detailed mechanistic model is lacking.

The newest addition to the retrograde movement model suggests OSM-3 and kinesin-II may directly transport IFT dynein, independently of the IFT particle in *C. elegan.* [11] The conclusion is derived from IFT-dynein undergoing normal IFT transportation speeds despite the uncoupling of IFT complex A/kinesin-2, and complex B/OSM-3. Another novel concept suggests IFT172 may mediate the interaction between inactivated dynein and the IFT particle during anterograde movement.[34] Additionally, a recent study in *C. elegans* revealed the presence of a novel retrograde dynein motor, specific to outer labial quadrant neurons, which are able to form full functional cilia in canonical IFT dynein mutants.[11]

**The IFT Particle**

By comparing the flagellar proteome of a *fla10*$^{ts}$ mutant after incubation at the non-permissive temperature to the wild-type flagellar proteome, Cole and colleagues biochemically observed the depletion of some proteins from the flagellar compartment.[5] After further analysis, members of the IFT particle were discovered. Results from this

study also revealed the IFT particle was actually comprised of two sub-complexes, IFT-A and IFT-B, which to date consist of 6 and 12 polypeptides, respectively.[20] A recent study revealed the structural organization of the IFT-B subcomplex, and demonstrated that it can be further separated into two tetrameric subdomains: IFT25/27/74/81/72 and IFT52/46/88/70.[35-37] IFT52 was shown to function as the interface between the IFT74/81 and IFT52/46/88/70, while IFT74/81 serves as the intermediate bridge between IFT25/27 and IFT52/46/88/70. The IFT-A complex is understood to be composed of IFT144/121/140/121/139/43[33]; a recent study uncovered the structural arrangement of the IFT-A complex.[38]

A majority of the IFT members are enriched in WD40 and tetracopeptide repeats (TPR), multi-protein binding domains that possibly form a circularized beta-propeller structure and alpha helical solenoid, respectively. These binding motifs are thought to function as scaffolding elements for IFT sub-complex assembly.[20] WAA is another binding motif present in IFT proteins, though the nature of the motif it is poorly understood. IFT core proteins contribute to the overall structural integrity of their respective sub-complexes, evident by the subsequent instability and cytoplasmic depletion of complex-mates following disruption of the core proteins. Flagella morphology is typically affected in one of two ways depending on which complex is compromised: structurally sound but severely truncated cilia (IFT-B mutants) or short bulbous flagella filled with electron dense clots (IFT-A).[1,13,31] The resulting phenotypes reveal the how the two complexes contribute differently to ciliogenesis. The short

flagella in IFT-B mutants suggest IFT-B operates in anterograde movement and the protein buildup in the flagella compartment in IFT-A mutants is reminiscent of retrograde IFT mutants (Fig. 3). Nonetheless, the many parts of IFT machinery must work in a concerted effort to strike an efficient balance between retrograde and anterograde transportation dynamics.

**IFT Complex A**

The function of individual IFT-A sub-complex proteins are mostly unknown. Much like the IFT-B complex, disruption or depletion of a single IFT-A protein leads to the instability of the complex and subsequent depletion from the cell body.[34] Mouse IFT122 was shown to regulate members of the sonic hedgehog pathway in a number of ways by affecting the localization of certain proteins differently than IFT-A and IFT dynein mutants.[39] In *Drosophila,* ciliary TRPV ion channels were undetectable in IFT140 mutant on a Western blot; although the mRNA levels remained static, IFT140 may function in the post-translational stabilization of the ion channels.[40]

The more predominant understanding of the IFT-A function comes from its importance to retrograde movement. At the permissive temperature, electron-dense bulges are present within the cilia of temperature-sensitive *Chlamydomonas* mutants in IFT139 (*fla17*) and IFT144 (*fla15*). A shift to the non-permissive temperature leads to the complete breakdown of retrograde IFT, resulting in lolli-pop shaped bulbs filled with IFT-B proteins.[32,33] This phenotype was also observed in IFT dynein mutants, thought to arise from the possible hindrance of retrograde IFT activation, and ultimately leading

to the buildup of turnover products and IFT particles within the flagellar compartment.[41] In *C. elegans*, IFT-A directly interacts with kinesin-II while IFT-B is transported by OSM-3. IFT-A and IFT-B are linked together by the BBSome, a secondary adaptor complex important for ciliary membrane biogenesis.[23,42]

**IFT Complex B**

Defects in the IFT-B complex typically lead to a bald phenotype, making any biochemical analysis a challenge to determine the individual function of each IFT-B protein. Most IFT-B core proteins are currently only known to serve as structural components, though some have been experimentally shown to function as direct adaptors for specific flagella cargo. In the *ift46* mutant, IFT-B complex partially assembles the complex B core proteins although stability is severely affected, evident by the presence of structural sound yet short flagella in *Chlamydomonas.*[43] Further study showed IFT46 serves as an adaptor protein for the specific transport of ODA16, a component of the outer dynein arms.[44] A subset of IFT-B proteins could potentially function as mechanical components of an anchoring mechanism designed to facilitate the loading of IFT-B onto the transition zone. Mutant strain *ift88,* the first IFT protein to be implicated in disease [45], produces a structurally sound IFT-B complex that is unable to load onto the transition zone.[46] The absence of IFT54/MIP-T3 causes the entire IFT motor/particle complex, with the exception of OSM-3, to mislocalize in *C. elegans.*[26]

Additionally, there are also peripheral proteins associated with complex B: IFT57, IFT20, IFT172, and IFT80.[35] IFT20 is a particularly interesting protein, because it is the

only IFT protein that can localize to the Golgi apparatus. The current model suggests IFT20, using IFT57 as an intermediate to the IFT-B in zebrafish [47], is involved in directing vesicles transporting ciliary-specific proteins to the basal body, and participating in the trafficking of membrane proteins into the flagellar compartment.[48] IFT172 readily dissociates from the IFT particle and was shown to be important for retrograde movement. Using the temperature sensitive mutant *fla11*$^{ts}$ (IFT172), Pederson et al. 2006 concluded that IFT172 directly interacts with CrEB1, a protein exclusively located at the flagella tip, and accumulates IFT-B but not IFT-A nor IFT dynein proteins in the flagella.[41] Recently, evidence of IFT172 involvement in the flagellar entry of IFT-dynein was detected in *Chlamydomonas*. Upon incubation at the non-permissive temperature, IFT-dynein is depleted from the flagella compartment of the temperature sensitive IFT172 mutant while the rest of IFT particle remains at wild-type levels.[34]

**The Transition Zone**

As mentioned before, the transition fibers mark the entrance of the flagella compartment by tethering the plasma membrane to the base of the flagella. The ciliary proteome contains various proteins concentrated at levels not found in the cytoplasm, implying an inherent selectivity to the transition zone barrier (TZ).[49] Although the complete regulatory pathway remains poorly understood, various studies have begun to demonstrate the complexity of the flagella gating mechanism. Recent biochemical characterization of *cep290* mutant in *Chlamydomonas* revealed that the protein CEP290

functions as an intricate member of the TZ proteins.[50] CEP290 is part of the MKS/MKSR/NPHP proteins (Meckel-Gruber syndrome/related and nephronophthisis), shown to localize at the base of the flagella. Together these proteins form the transition zone and function as the ciliary selective barrier, evident by the accumulation of non-ciliary proteins in the cilia of various TZ mutants.[51,52] Although IFT anterograde movement was normal and retrograde slightly slower, the *cep290* flagella accumulated IFT-B proteins and BBS4, yet had a reduction of IFT-A, some membrane proteins and axonemal precursors. This phenotype suggests CEP290 plays a role in the mechanical selectivity of the TZ; it could be possible that IFT-B binding/priming at the transition zone requires CEP290, which could explain the mostly unhindered movement of IFT and the buildup of IFT-B and not IFT-A.

Additional selectivity mechanisms have become more apparent, such as the requirement of ciliary transport signal (CTS) for access to the flagella compartment.[53] The VxPx motif has been shown to be important for the targeting and entry of ciliary membrane proteins polycistin-1 and rhodopsin. In contrast, a recent study discovered a mechanism for molecular retention, whereby passive diffusion into the ciliary membrane is inhibited by a transferable retention signal.[54] Podoclayxin was shown to contain a four- amino acid PDZ binding motif that facilitated its interaction with NA+/H+ exchanger 3 regulatory factor NHERF1, a protein attached to the apical actin cytoskeleton.[55] The conserved four- amino acid sequence in the PDZ binding motif was shown to be sufficient to prevent passive diffusion into the ciliary membrane domain.[54]

Although the ciliary entry is passive, the ciliary membrane protein retention appears to require the protein to be firmly attached to the axoneme. Thus, a ciliary retention signal is likely to be necessary for membrane protein accumulation in the ciliary compartment. Additionally, much like the gating system for the nuclear pore complex, a RAN-GTP has been found to exist between the cilia and cytosol that is important for import of KIF17, via its Ran-GTP dependent association with importin-β2.[27]

**GTPases in Intraflagellar Transport**

Research in small GTPases has demonstrated various instances in which GTPases play a direct or supplementary role in the trafficking of the IFT particle. ADP-ribosylating factor–like 13 (ARL-13), BBS3 and the BBSome are involved in the targeting and entry of flagellar membrane proteins into the compartment.[53] ARL-13 and ARL-3 are small G-proteins antagonistically operating to maintain the stability of IFT particles during middle segment transport in *C. elegans* (IFT A and B).[56,57] ARL-13 may also have roles involved in maintaining axonemal integrity since null mutant animals have a variety of gross ciliary abnormalities.[56-58] It has been suggested that ARL13 may in fact regulate the coupling of IFT-A and IFT-B, while ARL3 regulates IFT-B interaction with OSM-3; together they regulate the integrity of the IFT machinery in *C. elegans.*[57] Rab8 is recruited to the transition zone by Rabin8 (Rab8GEF), following stimulation from BBS1, a core member of the BBSome; this ultimately results in the fusion of post-Golgi vesicles shuttling ciliary membrane proteins near the basal body.[59,60] Dominant negative and constitutive active constructs demonstrate the impact

that the nucleotide state of Rab8 has on its entry into the ciliary compartment and its role in ciliogenesis.[17] Arf4 and Rab11 form a complex with Arf GTPase activating protein ASAP1 and FIP3 to package and transport rhodopsin from the trans-golgi-network to photoreceptor cilia.[61] This interaction between rhodopsin and Arf4 is dependent on a VxPx motif, a ciliary localization signal also found in other ciliary membrane proteins.[53] Recently, the VxPx motif has been shown to be essential for the trafficking of polycistin-1 protein, and to be involved in the recruitment of Rab8, thereby promoting fusion of ciliary membrane protein-containing vesicles.[62] Another small GTPase, Rab23, was found to be responsible for the turnover of sonic hedgehog signaling protein, Smoothened, from the ciliary compartment.[63]

**IFT-particle Integrated GTPases**

Two mysterious members of the IFT-B complex, IFT27 and IFT22, are the only small GTPases known to directly interact with the IFT particle. IFT25 is a phosphoprotein of unknown function that serves as a binding and stabilizing partner to IFT27.[64] Partial depletion of the complex B subunit IFT27, a small GTPase with high sequence homology to Rab-like 4 (RABL4) [65,66], reduces the levels of both complex A and B proteins in *C. reinhardtii.*[65]\ Due to its categorization as a small GTPase, it is unlikely that IFT27 contributes as a structural component in the stability of the A and B complexes. Recent work on IFT27 confirmed its GTP binding and GTPase activity along with solving the crystal structure of the sub-complex IFT25/27. However, both the

mechanism and the pathway through which IFT27 regulates the cellular amount of IFT particles remain to be identified.

IFT22 has been the more controversial of the two, since in studies with *C. elegans* and *Trypanosome* IFT22 homologs produced conflicting results. *C. elegans* IFTA-2, the RABL5 homolog in *C. elegans*, was predicted to be a complex B-associated protein because it was observed to move together specifically with IFT complex B, when complexes A and B traffic separately.[67] A putative constitutive active form (GTP-locked) of the IFTA-2 (IFT22 homolog) can enter the ciliary compartment while dominant negative (GDP-locked) diffusely localizes throughout the neuronal cell body and is notably excluded from the ciliary compartment. The result suggests that only the GTP-bound form of IFTA-2 participates in active IFT traffic. [68] More importantly, the null IFTA-2 (IFT22) mutant had intact sensory cilia, effectively suggesting IFTA-2 is not essential to ciliogenesis. However, the IFTA-2 null mutants exhibited extended lifespans, reminiscent of insulin IGF-1-like signaling pathway defects, and a failure to enter dauer formation, conveying IFTA-2 regulates specific signaling activities in the cilia.[68] Conversely, the RNAi knockdown experiments in *Trypanosome* RABL5 lead to the buildup of IFT particles in the flagella compartment and subsequent shortening of the flagella.[69] This phenotype is similar to mutants with defective retrograde IFT [12,70,71], suggesting RABL5 is essential to ciliogenesis.

**Recent Developments in IFT22/RABL5**

A documented characteristic of IFT particle proteins is their dependence on the kinesin-II motor for transport into the flagellar compartment. Preliminary experiments used *C. reinhardtii* mutant *fla10-1* [72,73], a temperature sensitive (ts) strain harboring a point mutation in the kinesin-II motor subunit FLA10 [74], to determine whether the entry of IFT22 into the flagella is FLA10-dependent.[5,6] Ciliogenesis is functionally normal at the permissive temperature (18°C) though anterograde movement is abolished when shifted to the non-permissive temperature (32°C). The immunoblot in Figure 2A demonstrates the gradual reduction of IFT22 from the flagella compartment over the course of 2 hours; the zero point marks the temperature shift from the 18°C to 32°C. The pattern of IFT22 depletion mimics those of tested IFT-A complex protein IFT139 and the IFT-B complex proteins IFT81 and IFT46, confirming IFT22 requires the kinesin-II motor to gain entry into the flagella compartment. Additionally, a co-immunoprecipation using α-IFT22 antibody was used to determine if IFT22 physically interacts with other IFT particle proteins. Figure 2B clearly demonstrates the enrichment of both IFT-A complex IFT139 and IFT-B complex IFT81 (Fig 2B); kinesin-II subunit FLA10 and the dynein retrograde subunit DHC1b. The results suggest IFT22 is tightly associated with the IFT particle and IFT motors.

Following sucrose density centrifugation, complex A and complex B proteins from whole cell lysates settle into two distinct peaks near the 16S region.[64] This well-

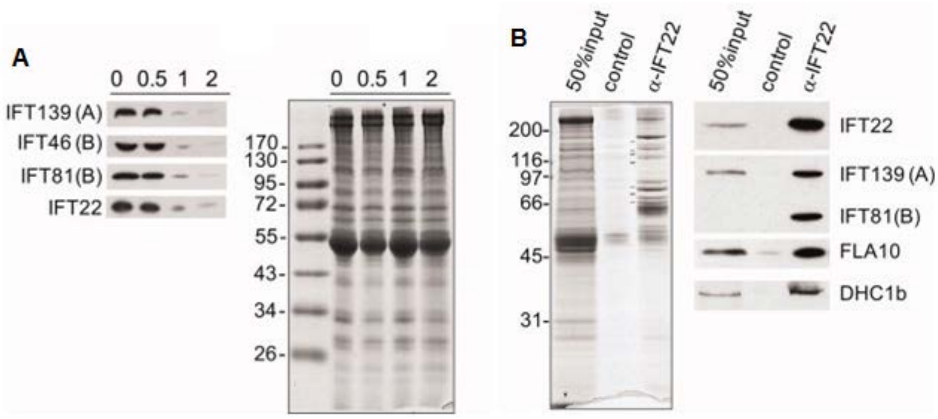


**Figure 2 IFT22 is an IFT protein.**[75]
Western blot depicts flagella time-course sample from *fla10*$^{ts}$ after incubation at 32°C. (0 to 2hrs) Coomassie Blue gels serves as loading control. **(B**) Immunoprecipitation was performed using IFT22 antibody against soluble flagellar proteins isolated from 32liters *cc125* culture. Control lane contains protein A-Sepharose beads only. Coomassie blue stain included.

established attribute allowed the initial classification of IFT particle proteins as distinct members of either IFT-A and IFT-B complexes.[5] In light of this, a sucrose density gradient focusing on the sedimentation pattern of IFT22 would definitively confirm whether IFT22 is an IFT-A or IFT-B protein. Preliminary work used wild-type protein extracts to perform the sucrose density gradient experiment depicted in Figure 3A, complex A subunit IFT139 and complex B subunit IFT81 sediment into two peaks, approximately two fractions apart. IFT22 peaks in the same fractions as IFT81, suggesting it is indeed an IFT complex B protein. Figure 3 Panel 2B contains the sucrose density gradient results from *ift88*, a mutant strain containing an insertional mutation within IFT-B complex protein IFT88[45]; IFT-B complex remains relatively intact. In the absence of IFT88, complex B proteins dissociate more readily and will sediment nearly four fractions away from IFT-A protein IFT139. IFT22 repeatedly co-sedimented with IFT46, further supporting the conclusion that IFT22 is a member of the IFT-B complex core proteins.

Typically, core IFT proteins contribute to the overall integrity of their respective sub-complexes. When IFT proteins are individually disrupted, either by mutation or artificially, complexes-mates are also negatively affected. We prepared protein extracts of a various IFT-A and IFT-B core protein mutants and performed a Western blot (Fig. 3) to monitor the expression levels of IFT22 when the IFT particle complex is compromised. The strains *ift46, bld1/IFT52,* and *ift88* were selected for their IFT-B mutant backgrounds. The *cc125* strain represents the wild-type control; *bld2* (defect in

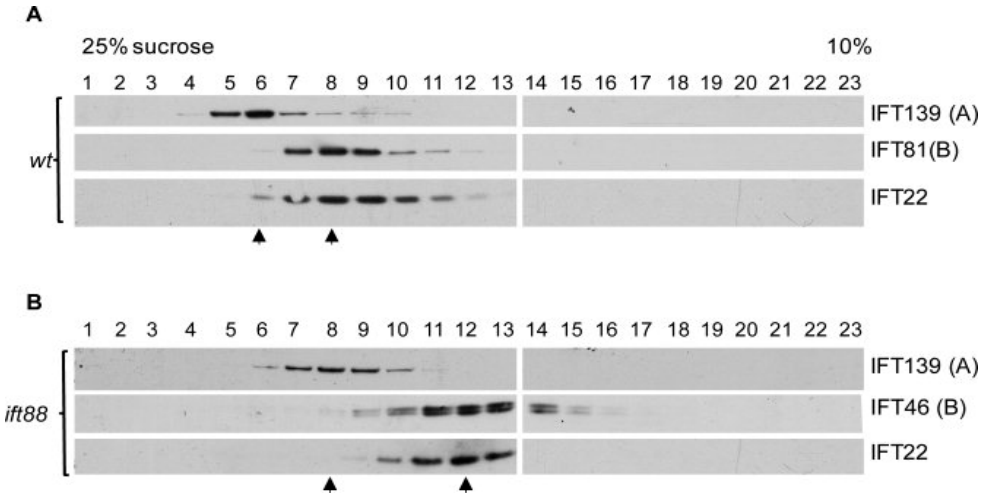


**Figure 3 IFT22 co-fractionates only with complex B on sucrose gradients.**[75]
Whole cell lysates from wild-type cc125 (panel A) and ift88 mutant (panel B) were fractionated through a 12-mL 10-25% sucrose density gradient. The resulting fractions were separated by SDS-PAGE and were analyzed by immunoblotting using antibodies of IFT139 (A), IFT81 (B), IFT46 (B), and IFT22.

basal body; flagella-less) and *fla10null* demonstrate whether IFT22 levels are affected by the absence of an intact flagella or compromised motor, respectively. IFT-B proteins were significantly depleted in the IFT-B mutant backgrounds (Fig 4A) while IFT-A protein IFT139 expression levels were increased. IFT139 was also significantly depleted in *fla17-1* while IFT46 remained relatively unchanged in *fla15* and *fla17-1* strains, mutants for IFT144 and IFT139, respectively (Fig. 4B).[33] The results are consistent with previous reports [34,43,45,65,76] and demonstrates the overall contribution of IFT core proteins to their respective complexes and the need for all components to properly integrate in order to yield a structurally sound IFT particle. Remarkably, IFT22 remains unchanged in the IFT-B mutant backgrounds, suggesting it does not require an intact IFT-B complex to be stably expressed. Taken together with the IFT-A mutant data, the results show that depletion of either IFT-A or IFT-B affects the normal expression levels of IFT22.

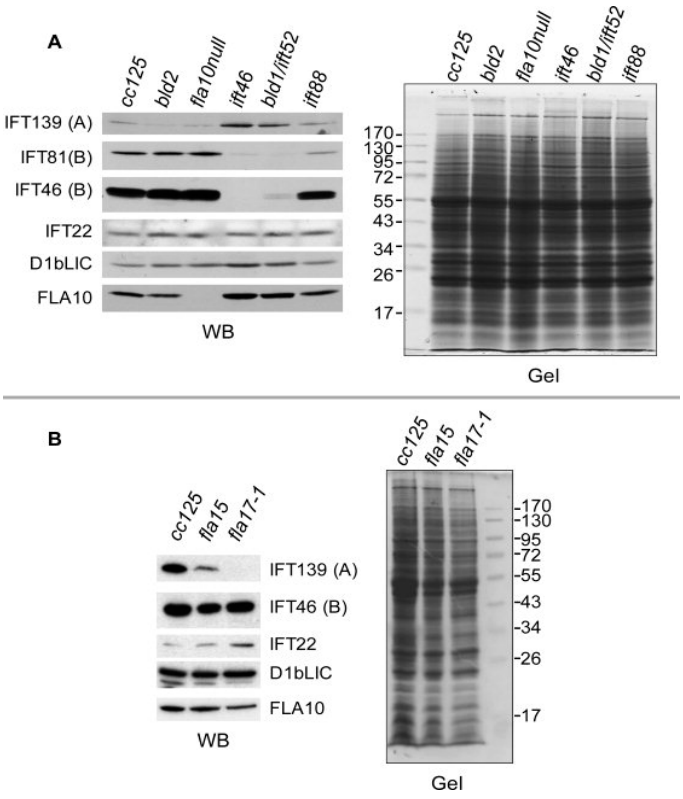


**Figure 4 IFT22 is stably expressed in IFT-A and IFT-B mutant backgrounds.** [75] Whole cell western blots of various IFT-B mutants (panel A) and IFT-A (panel B) have stable expression of IFT22. Coomassie blue stains depicted for loading control.

# CHAPTER II

# THE RABL5 HOMOLOG IFT22 REGULATES THE CELLULAR POOL SIZE AND THE DISTRIBUTION OF IFT PARTICLES INTO THE FLAGELLAR COMPARTMENT OF *CHLAYMDOMONAS REINHARDTII**

Cilia and flagella, sensory and motile structures protruding from the cell body, rely on the continuous bidirectional traffic of intraflagellar transport (IFT) particles to ferry precursors into flagella for assembly. Cells synthesize a large pool of IFT particle proteins in the cell body, but only a small portion engages in active transport within the flagella at any given time. The atypical small G protein Rab-like 5 (RABL5) has been shown to move in an IFT-like manner in the flagella, but its function in ciliogenesis is controversial. We previously demonstrated IFT22, the *Chlamydomonas reinhardtii* homolog of RABL5, is a *bona fide* IFT particle complex B subunit and remains stably expressed in IFT-B compromised mutants. In this thesis report, we report the depletion of IFT22 leads to a smaller pool of both IFT complex A and B proteins. We observed that a smaller cellular pool of IFT particles does not result in a reduced distribution of IFT particles to flagella or significant defects to flagella formation. Instead, the flagellar compartment undergoes an influx of IFT particle proteins, including IFT22 itself.

---

Moreover, cells over-expressing IFT22 also accumulate IFT particles in their flagella. Our data indicates that IFT22 controls the cellular levels of both complex A and B in *C. reinhardtii*, and thus plays a critical role in determining the cellular availability of IFT particles. Although it may not directly carry any precursors for flagellar assembly, IFT22 regulates how many IFT particles actively participate in ferrying precursors into flagella.

This chapter will also describe the construction of two artificial microRNAs optimized to target the non-coding 3' unstranslated region of IFT27 and the generation of a super-active variant of IFT22 produced through site-directed mutagenesis for *in vivo* and biochemically studies. Finally, we will also discuss preliminary data suggesting IFT25/IFT27 may function downstream of IFT22 to regulate the assembled IFT machinery complex including the IFT motors and BBS3.

**INTRODUCTION**

The IFT particle research has demonstrated how IFT-A and IFT-B complexes are distinct and structurally-independent entities within the IFT particle.[43] The stability of each complex has repeatedly been shown to depend on the proper integration of complex-respective subunits.[32,43,45,77] In addition to the self-contained regulation of each complex, the cellular amount of complex A and B has been shown to also be regulated concomitantly. Examples of IFT particle regulation are discussed in the IFT particle-integrated GTPases section of Chapter 1 ( [65] and this report).

Flagella are long and narrow structures where protein "traffic jams" can occur when an excessive accumulation of IFT particles or defective IFT-dynein can impede normal IFT trafficking along the axoneme. This particular scenario is observed in multiple retrograde-defective mutants [7,8,11,14,22,28,30,41,68,71] and RABL5 depleted *T. brucei*.[69] Normally, IFT particles concentrate at the peri-basal body region at the base of the flagella[78], and only a small portion of total IFT particles enter the flagella to undergo IFT.[64,79] This small, active portion of IFT particles is responsible for ferrying flagellar precursors from the cytosol to the flagellar compartment. Since ciliary proteins are synthesized in the cell body, and because the transition zone functions as physical barrier between the cell body and the flagellar compartment [50-52,80], the entry of precursors is understood to be a critical step in ciliogenesis [1,44] that must require an intuitive regulatory mechanism to control. Currently, little is known about how the size of the cellular pool of IFT particles is controlled or about how the number of IFT particles are allocated to active IFT is regulated.

To gain insights into the regulatory role of RABL5 in flagellar assembly, we have focused on the RABL5 homolog of *C. reinhardtii*, in which routine biochemical analysis of flagellar proteins is relatively easy. We previously identified an IFT particle protein IFT22 through biochemical purification and reported IFT22 as the *Chlamydomonas* homolog of RABL5.[64] Additionally we also determined IFT22 is an integral component of IFT particle complex B. In this thesis, we report the partial depletion of IFT22 specifically reduces the levels of both complex A and B proteins,

while the IFT motors remained relatively unaffected. In light of this, we conclude IFT22 regulates the cellular pool size of IFT polypeptides. Moreover, based on biochemical analysis of flagella isolated from cells expressing abnormal amounts of IFT22, we demonstrate IFT22 regulates the amount of IFT particles distributed to the flagella. These results provide new insights into how the cell regulates the partitioning of IFT particles between the cell body and the flagella.

## RESULTS

### The Cellular Pool Size of Complex A and B Are Simultaneously Reduced in IFT22 Knockdown Cells

An RNAi interference strategy was used to investigate whether depletion of IFT22 affects cellular levels of either IFT-A or IFT-B proteins in *Chlamydomonas*. Three constructs were designed and introduced into *cc125* wild-type cells: two constructs expressed long, double-stranded RNA targeting the either the coding region or the noncoding 3' untranslated region (UTR) of IFT22 (Xiaomeng Huang, unpublished). The third construct was designed as an artificial microRNA (amiRNA), optimized to target a sequence near the translation initiation site of IFT22 mRNA. Whole-cell extracts of transformants were prepared and analyzed for depletion of IFT22 by immunoblotting; each construct was transformed and screened four times, yielding over 600 individual transformants. Resulting immunoblots revealed the construct targeting the coding region of IFT22 was non-efficient, though the amiRNA and dsRNA with the 3'UTR target were highly effective in reducing the expression of IFT22.

Approximately 10% of the transformants achieved a 50% or greater reduction of IFT22 cellular levels. The knockdown effect of the amiRNA was more reproducible and stably maintained compared to transformants harboring the IFT22 3'UTR dsRNAi, and thus was selected as the primary RNAi construct for the remainder of the study. Transformants with an approximate 80% were selected for further analysis to determine the cellular condition of IFT particle proteins.

The cellular levels of IFT particle proteins and IFT motor subunits were measured by immunoblotting whole-cell extracts of IFT22 knockdown transformants. IFT particle proteins from both IFT-A and IFT-B sub-complexes exhibited a reduction in amiRNA knockdown cells, though they were observed to decrease to different extents (Figs. 5 A1 and 6A, results on the strain b8-46 in Fig. 8A). Retrograde IFT motor subunit D1bLIC was slightly reduced while the protein levels of anterograde IFT motor subunit FLA10 remained unaffected at the cellular level. The approximate extent of IFT protein depletion was determined by measuring immunoblot band intensity relative to wild-type protein extracts (Fig. 5A3). The reduction of both complex A and complex B proteins in the IFT22 knockdown cells indicated that IFT22 is essential in maintaining the normal cellular levels of IFT particle polypeptides.

**Knockdown of IFT22 Leads to an Influx of IFT Particles into the Flagella**

To examine the effect of IFT22 depletion on flagellar assembly, we measured the length of flagella in IFT22-knockdown strains (Fig. 5B-B1). No gross differences in flagellar morphology were observed. Strains *b8-8* and *b8-48* had normal

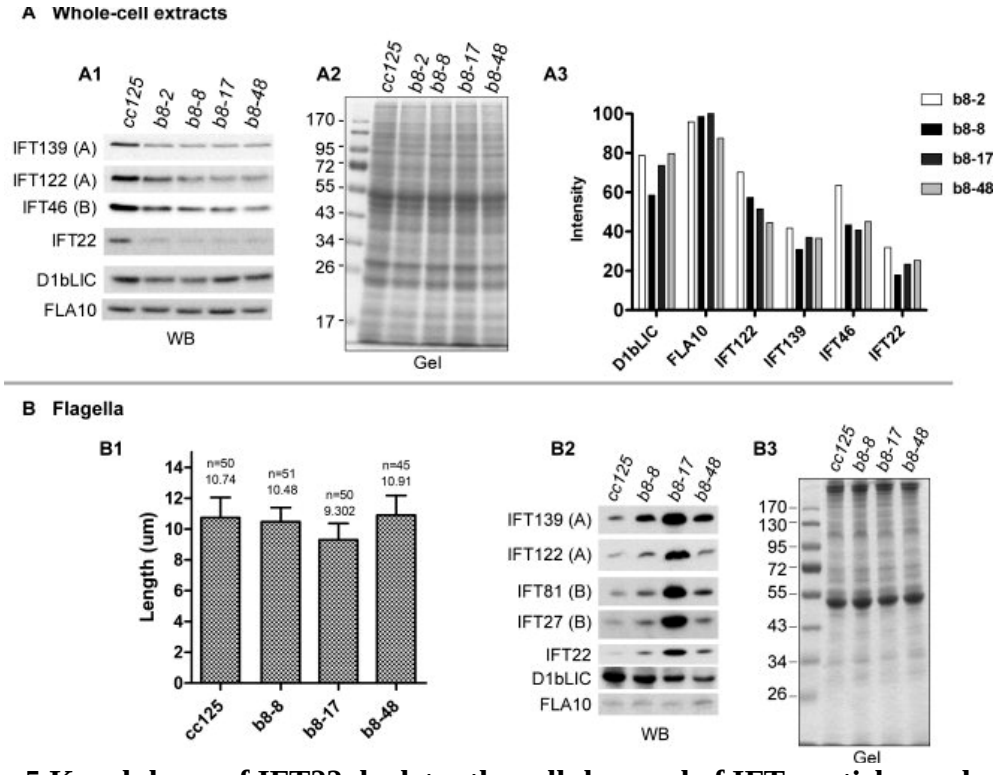


**Figure 5 Knockdown of IFT22 depletes the cellular pool of IFT particles and increases the distribution of IFT proteins into the flagellar compartment.**
Depletion of IFT22 leads to a smaller cellular pool of complex A and B (panel A), but an influx of IFT particles to flagella (panel B). (A1 and A2) Immunoblot analysis of whole-cell extracts showed IFT22-knockdown cells had reduced levels of IFT particle subunits, slightly reduced D1bLIC, and unchanged FLA10. (A3) Band intensities of the IFT particle proteins and IFT motors in the IFT22 knockdown strains from panel A1 were plotted as a percent of wild-type cells. (B1) Average flagella lengths of cells from wild-type *cc125* and IFT22-knockdown strains were compared. The mean length and the number of flagella measured are noted. (B2 and B3) The IFT22- knockdown cells accumulate IFT particle proteins, but not the motor proteins, in their flagella. Antibodies used against IFT proteins are as noted (A1 and B2). Equal loading of the samples is shown by the Coomassie Blue-stained gel in panel A2 and B3.

differences in flagellar morphology were observed. Strains *b8-8* and *b8-48* had normal flagella length though the flagella from the strain *b8-17*, were slightly shorter than wild-type (Fig. B-B1, *b8-17* mean length = 9.302 μm; wt = 10.94 μm, $p < 0.001$).

To address whether the knockdown of IFT22 led to a reduced distribution of IFT particles to flagella, we checked the levels of IFT particles and motors in flagella isolated from the three IFT22-knockdown strains. Strikingly, the flagellar amount of IFT particles was not reduced. Levels of complex A proteins, complex B proteins, and IFT22 were increased in the flagella of IFT22 knockdown cells, (Figs. 5B-B2, 5B-B3, and 8A). The flagella of *b8-17* were shorter than normal and experienced the greatest increase of IFT particles. The anterograde motor subunit FLA10 remained at the wild-type level and the retrograde motor subunit D1bLIC was slightly reduced (Fig. 5B-B2), or were unchanged (Fig. A). Collectively, these data showed that when the normal cellular expression of IFT22 is inhibited, more IFT particles, but not IFT motors, were distributed to the flagella compartment. The accumulation of flagellar IFT particles in IFT22-depleted cells is consistent with previous observations in RABL5-depleted *T. brucei* [69], suggesting IFT22 plays a conserved role in flagellar assembly.

**IFT22 Over-Expression Cells Contain Increased Amounts of IFT Particle Proteins in Both Cellular and Flagellar Compartments**

Unexpectedly, we observed an approximate 50% over-expression of IFT22 in 130 transformants generated via amiRNA (Fig. 6). To understand how the cells respond to a surplus of IFT22, we selected a few cell lines to analyze in detail (Fig. 6A).

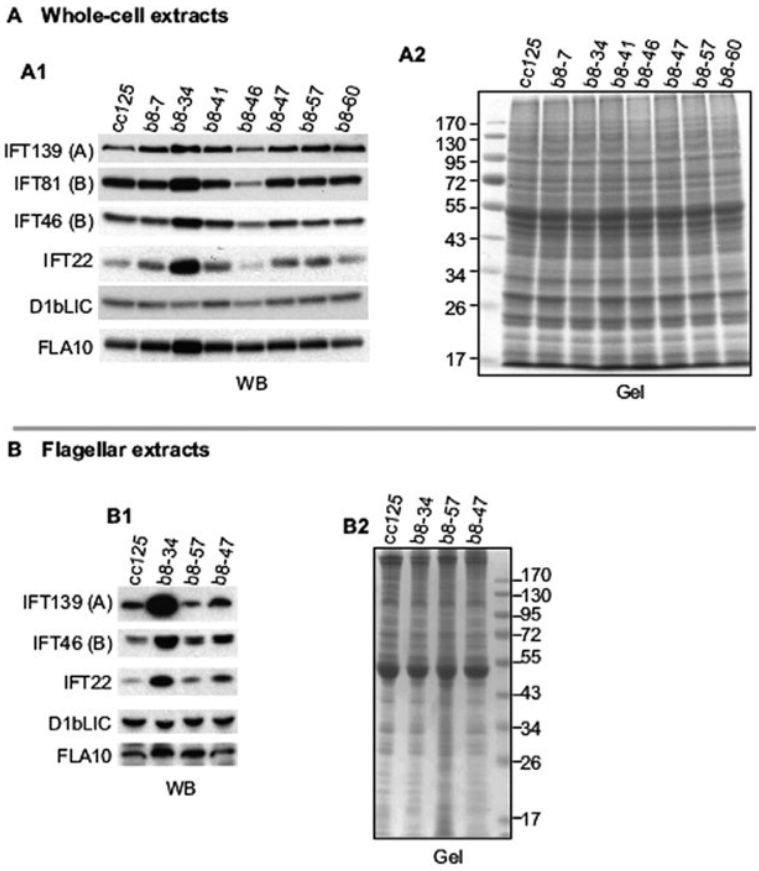


**Figure 6 Over-expression of IFT22 increases cellular and flagellar levels of IFT particle proteins.**

The whole-cell extracts (panel **A**) and flagella extracts (panel **B**) from the IFT22 over-expression strains were analyzed by immunoblot. (A1) Whole-cell extracts from cells of wild-type (*cc125*), over-expression strains (*b8-7*, *b8-34*, *b8-41*, *b8-47*, *b8-57*, and *b8-60*), and the knockdown strain (*b8-46*). (B1) The IFT22 over-expression cells accumulated IFT particle proteins in their flagella. Whole-cell and flagellar extracts from the over-expression strains were analyzed by immunoblotting proteins using noted antibodies. Equal loading of the samples is shown by the Coomassie Blue-stained gel in panel A2 and B2.

Immunoblot analysis of whole-cell extracts showed that the IFT22 over-expression strains had increased cellular levels of complex A protein IFT139. The amount of the IFT-dynein subunit D1bLIC was either unchanged or slightly reduced. Increased levels of complex B and the anterograde motor subunit FLA10 were also observed but were only prominent in strain *b8-34*, which experienced the most significant increase in IFT22 expression. These results indicated that over-expression of IFT22 upregulates the expression of IFT particle proteins. Moreover, this regulation affects IFT particle complexes A and B, and the IFT motor kinesin FLA10, but does not influence the expression of IFT-dynein.

The levels of IFT proteins were also measured in flagella isolated from several IFT22 over-expression strains (Fig. 6B). No obvious changes of flagellar IFT proteins were found in with strain *b8-57*, which only had a mild over-expression of IFT particles (Fig. 6A). However, a significant increase of IFT particle proteins were observed in the flagella isolated from both *b8-34* and *b8-47* strains. This was especially true for the *b8-34* strain which also displayed the highest levels of whole cell IFT particle proteins (Fig. 6A). Despite the dramatic changes to IFT particle proteins amounts, no change was detected for the IFT-dynein subunit D1bLIC, and only a mild increase was seen for FLA10. Thus, IFT22 over-expression increased the level of flagellar IFT particles within the cell body, but not IFT-dynein.

We also examined the flagella morphology of the over-expression strains under the microscope (Fig. 7). The flagella lengths of the strains *b8-57* and *b8-47*, which had

moderate over-expression of IFT22, were normal. Severe flagellar defects were observed in strain *b8-34*, which experienced the highest increase in IFT particles at both the cellular and the flagellar levels. The defects included short flagella and unequal lengths of a cell's two flagella (Fig. 7A). A close examination revealed that the short flagella were often swollen and formed membrane bulges along the lateral membrane and at the tip of the flagella (Fig. 7A). Similar membrane bulges, previously observed in the flagella of retrograde IFT mutants, were found to be due to aggregation of IFT particles.[7,14,28,32] Though not experimentally established, these aggregates are thought to jam the IFT traffic, block the precursor assembly site, ultimately inhibiting flagellar assembly.[7] The flagellar assembly defects in the strain *b8-34* are likely caused by a similar process. However, since *b8-34* was the only strain overexpressing IFT22 several folds, it remains unclear whether such a dramatic overexpression was solely due to the effect of IFT22 amiRNA. It should also be noted that the *b8-34* strain was the only one among the overexpression strains that displayed a flagellar assembly defect, thus the significance of IFT22 overexpression on flagellar assembly needs to be verified.

**IFT22 Artificial miRNA Acts at the Translational Level**

The sequence of the amiRNA of IFT22 targets the site of translation initiation, likely blocking translation initiation without triggering mRNA cleavage and decay.[81-84] To check if the artificial miRNA acts at the level of translation or of mRNA transcription or stability, semi-quantitative RT-PCR was performed on both the IFT22

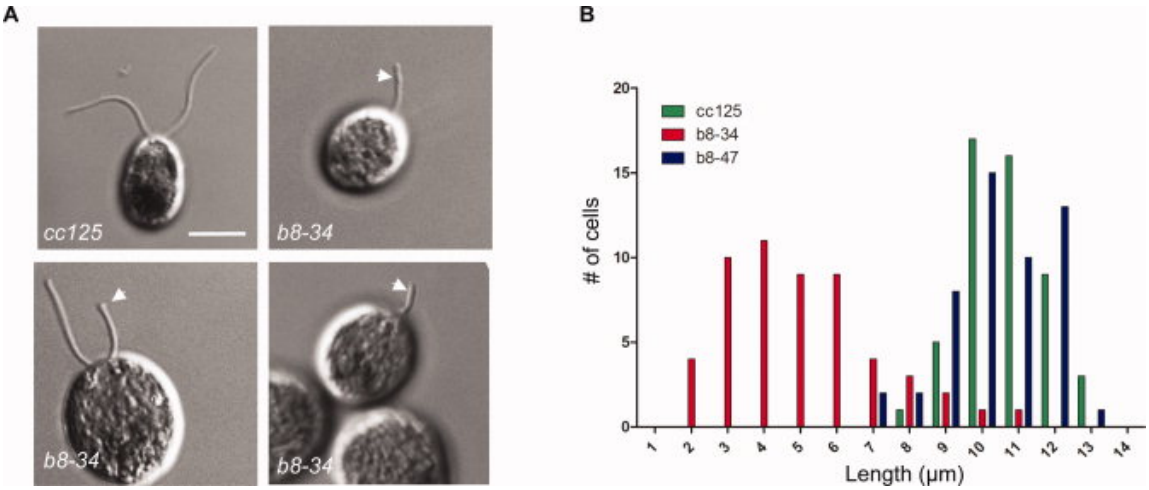


**Figure 7 Cells with several fold increase of IFT22 have severely shortened flagella fill with IFT particle proteins.**
(**A**) DIC images of wild-type *cc125* cells and *b8-34* cells. The flagella of *b8-34* cells were shorter than normal. Unequal lengths of two flagella were common in the population of *b8-34* liquid cultures. Membrane bulges (indicated as arrows) were also common at the flagellar tip or along the flagella. Scale bar, 5 μm. (**B**) Histograms showing the length distribution of flagella from wild-type *cc125*, and the over-expression strain *b8-34* and *b8-47* cells. The *b8-34* strain, which had several-fold increase of IFT22, had shorter flagella (mean length = 5.018 μm, $n$ = 54) compared to the *cc125* (10.72 μm, $n$ = 51) and the *b8-47* (10.39 μm, $n$ = 51) cells.

knockdown strains and the over-expression strains. The IFT22 knockdown strains *b8-17*, *b8-46*, which contained reduced cellular and elevated flagellar levels of IFT particle proteins (Figs. 5, and 6), had increased or unchanged levels of IFT22 and IFT27 mRNA compared to that of wild-type cells (Figs. 8). The over-expression strain *b8-34* had increased levels of IFT22 and IFT27 mRNA (Fig. 8). These data indicated that, in the case of IFT22, the repression via amiRNA was exerted at the step of translation instead of transcription, without major degradation of mRNA. The inhibition of translation likely induced a negative feedback that upregulated the production of IFT22 mRNA. The total level of IFT22 protein was therefore determined by the combined effects of miRNA inhibition and upregulation of transcription. Indeed, both silencing and over-expression effects were observed among the IFT22 miRNA transgenic lines.

**Constitutive Active IFT22 Enters the Flagella Compartment**

In order to establish the impact the predicted GTPase activity has on the trafficking of IFT22 into and out of the flagella compartment, several mutations were introduced into IFT22 to generate putative constitutive active and dominant negative (Xiaomeng Huang, unpublished data). The constitutive active variant was generated by mutating the P-loop glutamine at the $14^{th}$ amino acid to a valine (Q14V), and the threonine at the $19^{th}$ residue was replaced by asparagine (T19N) to yield the dominant negative form of IFT22. Additionally, each variant along with a wild-type IFT22 were supplemented with a HA and GFP tag in order to effectively detect the localization of

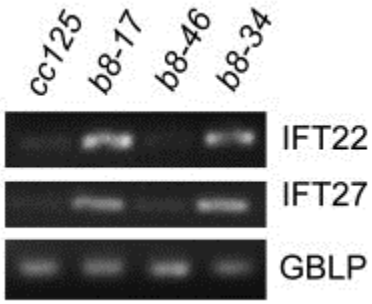


**Figure 8 Transcriptional levels of *ift22* and *ift27* amiRNA cell lines.**
Semi-quantitative RT-PCR was performed with RNA isolated from wild-type *cc125* and IFT22 amiRNA strains. DNA fragments of genes encoding IFT22, IFT27, and the β subunit of GBLP were amplified.

the IFT22 variants within the cell extracts. All three constructs were individually transformed into a *cw92* background, a mutant with a cell-wall defect in *C. reinhardtii,* permitting the use of a simpler transformation procedure. Over 50 transformants per variant were isolated following selection with varying degrees of transgenic IFT22 expression. Of those, a small group of representative transformants for each construct were selected for further testing.

In order to determine if the IFT22-Q14V and IFT22-T19N could successfully enter the flagella, cell body and flagella extracts were prepared and analyzed using immunoblotting. The IFT22:HA:GFP construct was detected in the flagella extract, suggesting the large GFP tag does not inhibit the trafficking of the transgenic IFT22 (Fig. 9). Much like the *C. elegan*s homologue IFTA-2 [68], IFT22-Q14V was detected in the flagella extract, thus confirming its entry the flagella (Fig. 9A). Compared to the wild-type IFT2, the constitutive variant had a smaller percentage of total expressed transgenic protein entering the flagella (Fig. 9A). To further verify the entry of the constitutive active IFT22, selected transformants were subjected to immunofluorescence. IFT22-Q14V properly localized to the basal body of the *cw92*, confirming its normal recruitment to the base of the flagella is not impaired (Fig. 9). Sporadic localization was observed throughout the axoneme, suggesting it may remain associated with the IFT particle when trafficking within the flagella compartment. Despite multiple transformations, the dominant negative variant would not sufficiently and consistently

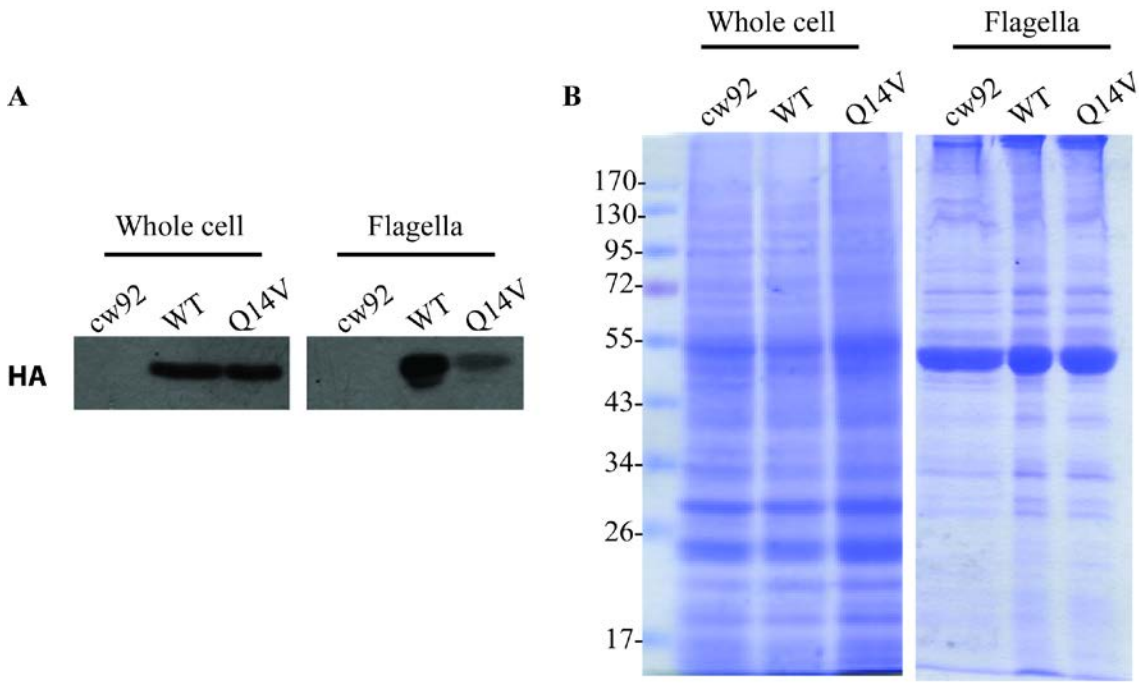


**Figure 9 IFT22 enters the flagellar compartment.**
IFT-GTP enters the flagellar compartment. Panel A contains immunoblots of whole cell and flagella extracts from selected transformants expressing IFT22-WT:HA:GFP and IFT22-Q14V:HA:GFP, denoted as WT and Q14V, respectively. A lower percentage of the GTP-locked IFT22 were shown to enter the flagella compared to the wild-type IFT22. Panel B shows the equal loading control of whole cell and flagella extracts using a Coomassie-Blue stain.

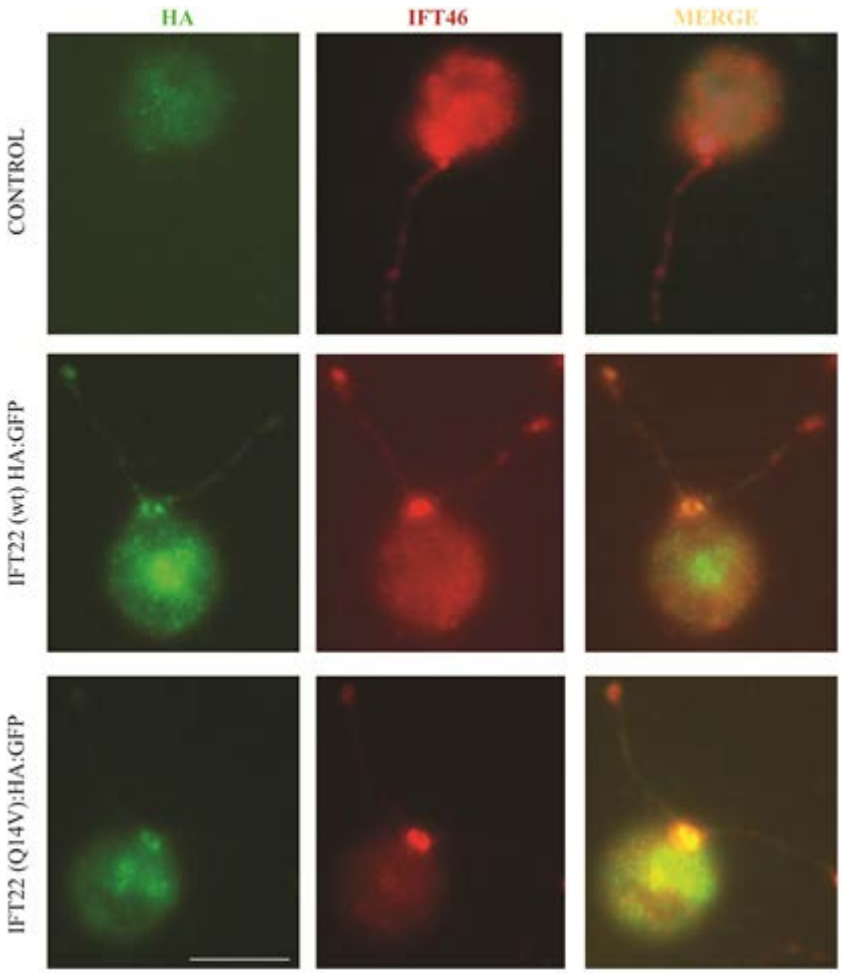


**Figure 10 Transgenic IFT22 and IFT22-GTP co-localize with IFT46 at the peri-basal body and flagellar compartment.**
The wild-type *cw92* cells were stained with anti-HA and anti-IFT46 antibodies. Both IFT22:HA:GFP and IFT22 (Q14V) HA:GFP localize to peri-basal body region concomitantly with IFT46. It should be noted that the reason for the high concentration of transgenic IFT22 and constitutive active IFT22 in the cytoplasm is unknown. Bar, 10 μm

express in *cw92* to permit the same biochemical verification procedures; as a result, further testing was not possible.

Both IFT27 and IFT22 have a serine residue on the 79$^{th}$ and 67$^{th}$ amino acid, respectively, in place of the canonical glutamine residue. Although GTPases have evolved multiple methods to achieving GTP hydrolysis, the glutamine to serine mutation in Rab-like proteins IFT27 and IFT22 was predicted to yield a lower GTP turnover rate. A recent study restored the canonical glutamine residue of IFT27 and observed a significant increase in GTP hydrolysis.[66] A super-active variant of IFT22 was constructed to be introduced into *C. reinhardtii* to observe its localization patterns and behavior *in vivo*. A mutation was introduced into IFT22 at S67→Q and supplemented with an HA tag for quick identification of successful transformants. Additionally, two constructs containing the IFT22 (S67Q):HA insertion were designed to add either a GFP for immunofluorescence and total internal reflection fluorescence (TIRF) microscopy experiments or His6 for future large scale purification. Additionally, paromomycin and bleomycin resistance markers were added to the GFP and His-tagged IFT22-S67Q construct, respectively. Generated plasmids were named as follows: pBluescriptIIKS+ift22 (S67Q): HA:GFP-PMM and pBluescriptIIKS+ift22(S67Q):HA:His6-Ble.

**Knockdown of IFT25 Results in Cytoplasmic Depletion of BBS3 and IFT motors**

A previous study and this thesis work observed the depletion of IFT-A and IFT-B proteins following the knockdown of IFT27 [65] and IFT22 in addition to their stable

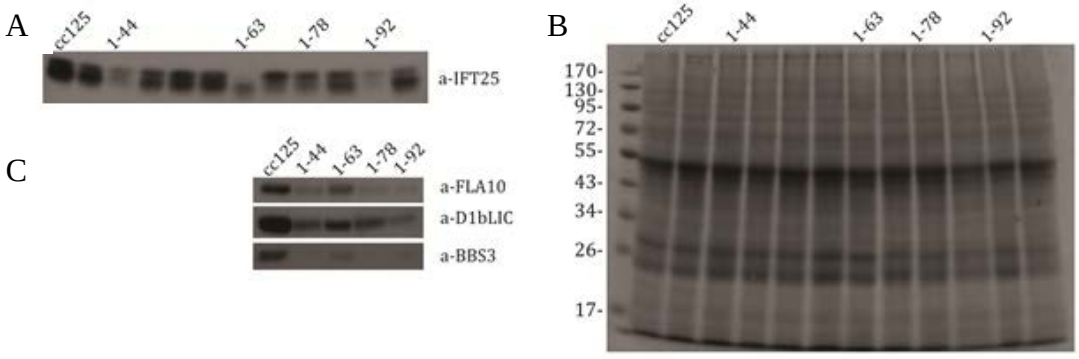


**Figure 11 Depletion of IFT25 leads to the depletion of IFT motors and BBS3.** Panel A is a whole cell extract immunoblot of IFT25 knockdown transformants with a range of IFT25 expression. Four transformants (panel A; *1-44*, *1-63*, *1-78*, and *1-98*) with lowest residual expression of IFT25 showed depleted levels of FLA10, D1bLIC and BBS3 (Panel C). Equal loading of the samples is shown by the Coomassie Blue-stained gel in Panel B.

expression in IFT-B mutant backgrounds. In an effort to determine whether IFT27 functions downstream of IFT22 or *vice versa*, an RNAi construct targeting the 3'UTR of IFT25 (Zhenchuan Fan, unpublished data), the binding partner of IFT27, was generated and transformed into *cc125* cells. Unfortunately, the results proved to be inconclusive as IFT22 protein levels would not follow a consistent trend in 25RNAi transformants (data not shown). However, selected transformants with an approximate 80% reduction of IFT25 (Fig 11A) replicating the results observed following knockdown of IFT27.[65] Surprisingly, BBSome subunit BBS3, kinesin-II subunit FLA10, and retrograde dynein subunit D1bLIC protein levels were also significantly depleted from the cell body (Fig. 11C). No significant defects were observed in the flagella of selected transformants with the highest level of IFT25 knockdown (data not shown). To verify the results, two artificial microRNAs were generated and optimized to target different regions of the IFT27 3'UTR using the same procedure employed in the building of the IFT22 artificial microRNA. Two constructs were generated and named as follows: pChlamiRNA3intIFT27-1 and pChlamiRNA3intIFT27-2.

## DISCUSSION

### Cellular Pool Regulation of IFT Particle Proteins

The *C. reinharditii* cell maintains a large pool of IFT particle proteins in the cell body[79], and only a small portion of the pool participates in active IFT within the flagella at any given time.[5] The pool size of complex B is approximately ten times larger than that of complex A [44], despite the fact that the assembled IFT particle from flagella has a

1:1 stoichiometry between complex A and complex B proteins. The difference in the pool size of complex A and B is thought to reflect the non-overlapping functions of these two complexes.[64] In this study, we show that IFT22 regulates the cellular pool of IFT particles, as reduced cellular levels of both complex A and B proteins are observed in IFT22 RNAi knockdown cells in *C. reinhardtii*. Thus, IFT22 is required to maintain the pool size of the IFT particle proteins, which in turn determines the availability of IFT particles.

This study describes an IFT22 over-expression strain which expresses IFT22 protein at levels several folds greater than normal (or wild-type) that also results in increases in complexes A and B and in FLA10. FLA10 is present at wild-type levels in various IFT particle mutants, including IFT22-knockdown strains, which all have reduced levels of IFT particles. Therefore, the cell has an apparent baseline level of anterograde motor FLA10, which is regulated independently of IFT particle production. The observation that FLA10 accumulates along with IFT particles upon over-expression of IFT22 suggests FLA10 can be positively regulated by responding to the surplus in the IFT-particle pool. In contrast, the expression of the retrograde motor IFT-dynein is insensitive to the changes of the cellular amount of IFT particles. The mechanism controlling the expression of IFT-dynein appears to be at least partially independent from control of IFT particle and FLA10 expression.

**IFT22 Regulates Amount of IFT Particles Distributed to the Flagellar Compartment**

Normally, the majority of IFT particles concentrate around the basal body and on the cytoplasmic side of the transition zone. As previous studies have shown, the cell only allocates approximately 20% of complex A and 2% of complex B to participate in active IFT transport within the flagella.[64,79] We observed partial depletion of IFT22 causes a decrease in the cytoplasmic pool of IFT particles. However, the absolute levels IFT particle proteins including IFT22 itself, actually increase within the flagella compartment. This build-up did not extend to IFT motors as both the anterograde motor subunit FLA10 and the retrograde IFT motor subunit D1bLIC displayed a normal distribution ratio between the cell body and the flagella. These results indicate that IFT22 is involved in regulating the specific distribution of IFT particles to the flagella.

The exact role of IFT22 in regulating the distribution of IFT particles remains unclear. Since the changes of IFT22 expression level also alter the cellular level of IFT particles, it is possible that the up-regulation of IFT A and B complex in the flagella in the IFT22 knockdown cells is simply due to the disruption of IFT particles. It is also possible that IFT22 is specifically involved in regulating the distribution of IFT particles. Nonetheless, the absolute amount of IFT22 cannot be the determining factor in the distribution of IFT particles, as both over-expression and depletion generate increased flagellar localization. We *hypothesize* that because IFT22 is a small GTPase, the

distribution or availability of IFT particles for IFT transport could potentially be determined by the ratio between the GTP-bound and GDP-bound forms of IFT22.

The *C. elegans* homolog of IFT22, when in the GDP-bound form, is excluded from the ciliary compartment, indicating that only the GTP-bound form is capable of entering cilia.[68] We also duplicated this result by biochemically confirming the presence of the constitutive active IFT22-Q14V within prepared flagella extracts. Since we observe a smaller percentage of the constitutive active variant detected in the flagella compartment, it is possible the endogenous IFT22 out-competes the transgenic IFT22-GTP for binding sites on IFT complex B. It is also possible that disrupting the normal GTP-GDP cycling of IFT22 impairs ability of the IFT particle/IFT-GTP locked complex to efficiently traffic into the flagella. Additionally, we also observed puncta localization throughout the axoneme, suggesting IFT22-GTP remains bound to the IFT particle while undergoing IFT within the flagellar compartment. Performing a sucrose density gradient of cell lines expressing the transgenic the constitutive active, dominant negative and super-active variants of IFT22 would definitively confirm whether the nucleotide status of IFT2 dictates its association with the IFT particle both in the cell body and the flagellar compartment.

Based on the data of previous studies and our own experiments, we *hypothesize* that the ratio between the GTP-bound versus GDP-bound IFT22 in the cell body is tightly controlled. The cell maintains this ratio by adjusting the number of IFT particles containing GTP-bound IFT22, which are the only version capable of entering the

flagellar compartment. Normally, only a small fraction of IFT particles would enter the flagella. However, as the ratio between the GTP-bound and GDP-bound IFT22 increases, the cell responds by sending additional IFT particles to the flagellar compartment in order to maintain. Increased amounts of flagellar IFT particles have been observed in IFT22-knockdown cells in *C. reinhardtii* (this thesis), *T. brucei* [69] and in the IFT22-over-expression cells in *C. reinhardtii* (this report). Based on our hypothesis, the ratio between the GTP-bound and GDP-bound IFT22 should increase in cells that express abnormally low or high amounts of IFT22.

This hypothesis also provides a reasonable explanation for the observation that the *C. elegans* IFTA-2 null mutant does not display an obvious defect in ciliogenesis or IFT [68] but rather defects in specific signaling activities within the cilia. The absence of IFTA-2 may alter the distribution of IFT particles to the cilia, which in turn could change the levels of some ciliary signaling molecules. However, such changes in the numbers of IFT particles would not have to disrupt the balance of anterograde and retrograde IFT to such a degree as to cause an obvious defect in ciliary assembly. Future research will be needed to establish the effect of GTP-bound and GDP-bound IFT22 on localization of IFT particles to the cilia and flagella.

**IFT25 May Regulate the Assembled IFT Particle/Motor/BBSome Complex Downstream of IFT22**

This work and a previous study [65] have shown that the depletion of both IFT22 and IFT27 results in a reduction of both IFT-A and IFT-B complex proteins. Our over-expression and knockdown of IFT22 significantly depleted the expression levels of IFT

particle proteins while the protein levels of kinesin-2 and IFT dynein-2 subunits were comparatively unaffected. Conversely, our knockdown of IFT25, the stabilizing partner of IFT27, resulted in the depletion of not only IFT particle proteins, but also both the retrograde and anterograde motors along with BBSome subunit BBS3. Previous studies have suggested IFT25/27 could be involved in the regulating the entry of the IFT machinery in the flagella compartment[64], though its impact on ciliogenesis may be species-dependent. Null IFT25 mutant mice were non-viable but tested positive for cilia formation; defects in Hedge-hog signaling were determined to be the cause of death.[85] Interestingly enough, the source of the signaling defects was the abolished trafficking of notable Hedgehog proteins including Patched-1, Smoothened, and Gli2 [85], suggesting IFT25 is also involved in the trafficking of ciliary membrane proteins. BBS3 itself does not contribute to the structural integrity of the assembled BBSome, however it is important for the recruitment of the BBSome to primary cilia.[86] Currently the only known direct interaction between the IFT particle and the BBSome is between *C. elegans* DYF-2, IFT-A protein IFT144 in *C. reinhardtii*, and BBsome core protein BBS1.[87]

Taken together, the data suggest IFT25 may be directly or indirectly involved in regulating the assembled IFT particle/motor/BBsome complex or the interaction between the BBSome and the IFT particle. Biochemical pull-down assays and direct interaction assays between IFT25 and the BBSome would definitively reveal if IFT25 serves as bridge between the BBSome and the IFT particle. It is tempting to speculate the recently

confirmed GTPase activity of IFT27 could serve as the regulatory trigger to control the assembly or loading of the entire IFT particle/motor/BBSome complex prior to the entry of assembled complex into the flagella.

## MATERIALS AND METHODS

### Strains and Culture Conditions

*Chlamydomonas reinhardtii* wild-type strain *cc125*, mutant strains, *ift88* (CC-3943) [45], *ift46* [43], *bld1/ift52* (CC-477) [76], *fla10* null (CC-4180) [21], *bld2* (CC478) [88], temperature-sensitive (ts) flagella assembly mutants *fla10*$^{ts}$ (*fla10-1* allele, CC-1919), *fla15* (CC-3861), and *fla17*-1 (CC-3862) [32,33,70] were obtained from the *Chlamydomonas* center (http://www.chlamy.org). The *ts* mutants were cultured on Tris-acetate-phosphate (TAP) solid plates or in M1 liquid media with constant aeration in a Conviron programmed at 18°C with a light–dark cycle of 14:10 h. Other strains, if not otherwise specified, were grown on TAP solid plates or in TAP liquid media at 22 °C in continuous light with constant aeration.

### Antibodies

Bacterial-expressed N-terminal $His_6$-tagged full length IFT22 recombinant protein (pTrcHis vector, Invitrogen) was used as the antigen for polyclonal antibody production in rabbits (The Woodlands, TX). Aliquots of immune serum were tested against blots of diluted recombinant IFT22 and sucrose gradient-purified IFT proteins to verify the avidity and specificity of the serum. Anti-IFT22 antisera were affinity purified from the GST-IFT22 proteins bound to the nitrocellulose membrane (Protran BA83, 0.2

mm, Whatman, Dassel, Germany). GST-IFT22 full-length fusion protein was made from the pGEX-2T vector (GE healthcare), and purified before being used for purification. Other antibodies used in this study include antibodies against α-tubulin (clone B-5-1-2, ascites fluid; Sigma), IC69 (clone 1869A; Sigma), Antibodies against *C. reinhardtii* proteins IFT25 [64], IFT27 [65], IFT139, IFT172, IFT81 [5], IFT72 [35], IFT46 [43], FLA10 [5], DHC1b [8] and D1bLIC [28]were also previously reported. Polyclonal antisera were raised against *Chlamydomonas* IFT122 in rabbit and will be described at a later time.

**Plasmid Construction and Chlamydomonas Transformation**

The miRNA construct pChlamiRNA3int-*ift22* was created as detailed previously.[89] The target sequence of *ift22* was scanned via http://wmd2.weigelworld/cgi-bin/mirnatools.pl for potential artificial miRNA target sites, and a 21-bp sequence (TCTATCTTCAACCCGTGCTGT) targeting the ift22 exon 1, the sequence right after the translation initiation codon, was chosen for further study. Two 90-mer oligonucleotides (*ift22*-ami-forward: 5′ ctagtACAGCACGGGTTGAAGTTA GAtctcgctgatcggcaccatgggggtggtggtgatcagcgctaTCTATCTTCAACCCGTGCTGTg 3′ and *ift22*-ami-reverse: 5′ ctagcACAGCACGGGTTGAAGATAGAtagcgctgatcaccaccaccccatggtgccgatcagcgagaT CTAACTTCAACCCGTGCTGTa 3′, Invitrogen) containing the targeted sequence in opposite directions separated by a 42-mer spacer sequence (lower case) were annealed *in vitro* and treated with T4 polynucleotide kinase (PNK, Fermentas) for phosphorylation. The miRNA vector pchlamiRNA3int was digested with SpeI (Fermentas) followed with

CIAP (Fermentas) treatment for dephosphorylation. The 90-bp DNA oligo was digested with SpeI and inserted into the pchlamiRNA3int vector. The correct miRNA colony was screened by nucleotide sequencing.

The construction of the IFT27 miRNA followed the same procedure denoted above; two 21-bp sequences located in the 3'UTR of IFT27, 5' TATCATTACATAAGCAGACAC 3' and 5' TCTTAGACCGGGATCTCTCAT3,'were designated as optimal targeting sites for the miRNA construct. The following pairs of 90-mer oligo nucleotides were used to generate constructs pChlamiRNA3int-ami27-1 and pChlamiRNA3int-ami27-2: ( **ami27-For_1** 5' ctagtGTGTCTGCTTATGTAAAGATAtctcgctgatcggcaccatgggggtggtggtgatcagcgctaTA TCATTACATAAGCAGACACg 3' and **ami27Rev_1** 5' ctagcGTGTCTGCTTATGTAATGATAtagcgctgatcaccaccacccccatggtgccgatcagcgagaT ATCTTTACATAAGCAGACACa 3); the second pair consists of (**ami27For_2** 5'ctagtATGAGAGATCCCGGTCAAAGAtctcgctgatcggcaccatgggggtggtggtgatcagcgcta TCTTAGACCGGGATCTCTCATg 3' and **ami27Rev_2** 5'ctagcATGAGAGATCCCGGTCTAAGAtagcgctgatcaccaccacccccatggtgccgatcagcgaga TCTTTGACCGGGATCTCTCATa 3', Invitrogen).

Constructs, pBluescriptIIKS+-ift22 (QV) HA- GFP-PMM and pBluescriptIIKS+-ift22 (TN) HA- GFP-PMM were generated prior to the initiation of this thesis work (Xiaomeng Huang, unpublished data). The construction of the pBluescriptIIKS+ift22 (S67Q)HA:GFP-PMM and pBluescriptIIKS+ift22 (S67Q)HA:His6 consisted of excising

full gene of IFT22, including endogenous promoter, coding region plus a HA tag, from the pBluescriptIIKS+-ift22 HA- GFP-PMM using a double digest reaction of Not1 and EcoR1. The IFT22:HA fragment was then inserted into a pGEM vector also digested by prepared by the Not1 and EcoR1, thereby forming the construct pGEM ift22:HA. The S67→Q mutation was introduced using the QuikChange Site-Directed Mutagenesis Kit (Stratagene) according to the manufacturer's instructions with the following parameters: 16 cycles; 95ºC (30secs); 55ºC (1min); 68ºC (11min); 4ºC (storage). Mutagenesis was carried out using primers ift22-S67Q-F (5' - GGA CGT GTC GGG GCA GGT GCA GTA CCA G - 3') and ift22-S67Q –R (5' - CTG GTA CTG CAC CTG CCC CGA CAC GTC C – 3'); following mutagenesis, the resulting construct was sequenced and confirmed for production of pGEM-ift22(S67Q):HA. The ift22 containing the super-active mutation plus HA tag were excised from pGEM-ift22(S67Q):HA using a Not1/EcorR1 double digest and subjected to a secondary digest of Sca1 to break the pGEM vector. The ift22(S67Q):HA fragment was isolated by gel purification and inserted into Not1/EcoR1 prepared and isolated pBluescriptIIKS+ -GFP-PMM and pBluescriptIIKS+ His6-Ble vectors. The resulting constructs containing a GFP and His6-tagged IFT22-S67Q variant were named as follows: pBluescripIIKS+ift22(S67Q):HA:GFP-PMM and pBluescripIIKS+ift22(S67Q):HA:His6-Ble, respectively.

**Whole-Cell Extracts Sample Preparation for Direct Electrophoresis Analysis**

When only small samples were needed, extracts were prepared from 1 ml of cells grown to log phase in TAP medium. After removing supernatant, the cell pellets were resuspended with 54 µl of Buffer A (0.1M $Na_2CO_3$), 6 µl of DTT and 40 µl of Buffer B (5% SDS, 30% sucrose), followed by vortexing for 45 min at 20 °C. Samples were spun down at 10,000 rpm for 5 min, and the supernatant was collected. 50 µl of each protein sample was mixed with 40 µl of water and 10 µl of 10X Laemmli buffer. The samples were mixed well by vortexing for 10 sec. Samples were then boiled for 3 min, followed by a brief spin, before loading for SDS-PAGE. When larger amounts of protein were needed, the sample size and the extraction solution were increased proportionally. The protein concentration of the samples was first measured by the Amino Black method, as previously described [65], and then adjusted based on the total intensity of the lanes stained by Coomassie Blue measured using the Image Lab™ Software (Bio-Rad).

**SDS-PAGE and Immunoblotting Assay**

Protein samples in 1 × Laemmli buffer were separated by 10% SDS-PAGE and then electrotransferred onto a nitrocellulose membrane (Protran BA83, 0.2 mm, Whatman, Dassel, Germany). Before immunoblotting, the membrane was stained with Ponceau S to ensure that proteins were properly transferred. Thereafter, the membrane was blocked with 5% nonfat dry milk in TBS (10 mM Tris, pH 7.5, 166 mM NaCl) plus 0.05%Tween-20. Primary antibodies were diluted in the blocking solution and then incubated with the membrane overnight at 4°C. After washing three times with TBS plus

0.05% Tween-20, horseradish peroxidase-conjugated secondary antibodies (Pierce Biotechnology, Rockford, IL) were incubated with the membrane for 1 h followed by washing three times with TBS plus 0.05% Tween-20. Chemiluminescence was used to detect the primary antibodies. The intensities of the immunoblot bands were quantified by the Image Lab™ Software (Bio-Rad).

**RNA Isolation and Reverse Transcriptase (RT)-PCR Analysis**

Total cell RNA from wild-type *cc125* and amiRNA cells was purified with TRIzol (Invitrogen) according to the manufacturer's instructions followed by DNase I (RNase-free) (Fermentas) treatment to remove contaminating DNA. RNA samples were purified by RNeasy Mini Kit (QIAGEN), and the concentration was determined by NanoDrop. Reverse transcription reactions were carried out with equal amounts of RNA from each sample using SuperScript III Reverse Transcriptase (Invitrogen), according to the manufacturer's instructions, with oligo (dT)20. By using the resulting cDNA as the template, fragments containing sequences from the genes encoding IFT22, IFT27, and the beta subunit of G protein-like protein (GBLP), which was used as a control for equal amounts of input RNA, were amplified by PCR. A fragment of 118 bp containing exon 4 and 5 of the *ift22* sequence was amplified with the primer IFT22qPF1 (5′-CAGT CTTACGTGGCCATCAA-3′) and primer IFT22qPR1 (5′-GGACGTCCAAATGCGAGTAT-3′). A 110 bp fragment containing sequence from *ift27* was amplified with the primer 27QPF2 (5′-TCTCGGTGGAGCTC TTTCTG-3′) and primer27QPR3 (5′-GCTCACA TCGAACACGAGAA-3′). A 141 bp fragment of

containing sequence from *gblp* was amplified with the primer GBLP3 (5′-GTCATCCACTGCCTGTGCTTCT-3′) and primer GBLP4 (5′-GGC CTTCTTGCTGGTGATGTT-3′). Five microliter of PCR product from each sample was used for 0.8% agarose gel electrophoresis.

**Microscopy and Phenotype Assay**

Wild-type *cc125* and IFT22 amiRNA cells were cultured in TAP liquid media and grown to log phase. A hundred microliters of cells were taken at the same time of the same day and then fixed by 1 × Lugol's iodine solution. Following the fixation, preparations were quickly photographed by the Olympus IX70 Inverted Microscope and Simple PCI Imaging System at 100× magnification. The lengths of flagella from 134–164 randomly selected cells from each strain were measured using ImageJ (http://rsbweb.nih.gov/ij/). Student's *t* test analysis of length data was performed using JMP®, Version 9.0., SAS Institute, Cary, NC, 2010. The data was processed with GraphPad Prism 5 (GraphPad Software), and flagellar lengths are presented as mean value (μm).

**Immunofluoresent Microscopy**

The same method described previously [90] was used. The primary antibody α-HA was purchased from Roche and used at a 1:25 dilution, IFT46 was used at a 1:200 dilution, the secondary antibodies were chosen according to the suggestions of the manufacturer. An Olympus IX-70 inverted fluorescence microscope at 100×

magnification was used to observe the staining and the images were captured by the PCI software package through an Image Point CCD camera (Photometrics)

# CHAPTER III

## SUMMARY AND CONCLUSION

The purpose of my thesis project was to investigate the mechanisms involved in regulating the entry/exit of IFT particles from the flagellar compartment, and how these mechanisms contribute to ciliogenesis.

In Chapter II, I demonstrated how depleting or over-expressing IFT22 in *C. reinhardtii* using an artificial microRNA resulted in a reduction or increase of the available cellular pool of IFT particles, respectively. Surprisingly, both the depletion and over-expression of IFT22 caused an influx of IFT particles into the flagella compartment. Using a transgenic IFT22 mutant, I showed that the IFT22 GTP-bound properly localized to the peri-basal body, enter the flagella and is likely to remain associated with the IFT particle while undergoing normal IFT trafficking in the flagella. Additionally, I demonstrated how the knockdown of IFT25 using RNAi resulted in a reduction of the cellular amount of BBsome subunit BBS3, kinesin-II subunit FLA10 and IFT dynein-2 subunit D1bLIC. Taken together, the data suggests IFT22 and IFT25, possibly in conjunction with IFT27, function in a sequential regulatory mechanism where IFT22 specifically regulates the availability of IFT particle for IFT trafficking and IFT25/IFT27 may directly or indirectly regulate the fully assembled IFT machinery prior to its entry into the flagellar compartment.

This thesis provides valuable insight into a potentially novel mechanism involved in regulating the sequential assembly or loading of IFT particle/motor/BBSome complex prior to the entry of IFT machinery into the flagellar compartment.

**FUTURE DIRECTIONS**

The IFT and cilia field in general has experienced a surge in interest after it was discovered that human genetic diseases, now collectively known as ciliopathies, are linked to defects in ciliogenesis. There are still many unexplored questions in the IFT community and thus many areas that could benefit from further study. In this section, I will address future directions that could use my work as a foundation for studies investigating regulatory mechanisms involved in the maintenance and trafficking of the IFT machinery. A recent study confirmed the GTP binding and GTPase activity of IFT27, an integrated protein of the IFT particle.[66] In the same light, confirming GTPase enzyme activity of IFT22 would be beneficial to understanding the function of IFT22. In the same study, researchers restored a canonical glutamine important for enzyme activity that is mutated to a serine in IFT27 and observed a significant increase in GTP hydrolysis.[66] Since IFT22 has the same serine residue as IFT27 and is likely to have low intrinsic GTPase activity, it is logical to assume there is potential GAP that facilitates that GTP hydrolysis activity of IFT22. Exploratory pull-down assays may lead to the discovery of IFT22-GAP that would be an important component to IFT particle regulation. It is currently unclear if the nucleotide status of IFT22 regulates its association with the IFT particle or if it is constitutively bound to IFT-B complex.

Performing a sucrose density gradient against cell extracts containing putative constitutively active, dominant negative and super-active variants of IFT22 would definitely confirm whether IFT22 is constitutively associated with the IFT particle. This scenario would support my hypothesis of the nucleotide status of IFT22 serves as a signaling beacon for the marking or targeting of the IFT particle for assembly with the remaining components of the IFT machinery. Although this information would support our hypothesis of IFT22 regulating the IFT particle pool through its GTP-GDP cycling, it does not convey whether IFT22 remains bound to the IFT particle throughout normal IFT trafficking within the flagella compartment. We have already demonstrated that the GFP tag on IFT22:HA:GFP does not hinder its recruitment to the peri-basal body region or its entrance into the flagella compartment. Using TIRF microscopy, it would be possible to track transgenic IFT22 variants during *in vivo* IFT trafficking within the flagella to determine if IFT-GTP remains associated with the IFT particle during IFT.

My amiRNA analysis showed that IFT22 regulates the cellular pool of IFT particles and the IFT particle distribution profile between the cytoplasmic and flagella compartment. An obvious shortcoming of RNAi studies is that the endogenous proteins levels are not completely eliminated. The discovery of an IFT22 null mutant could be used for rescue experiments using not only wild-type IFT22 but also the constitutive active, dominant negative and super-active variants of IFT22. The *in vivo* behavior of the IFT22 mutants and their impact on the ciliogenesis would provide a clearer picture of IFT22 true function in IFT particle regulation.

The influence of IFT25 over the cellular protein levels of FLA10, D1bLIC and BBS3 require more extensive research. My proposed use of IFT27 amiRNA would reinforce our current RNAi data for IFT25 knockdown strains but it will not reveal whether IFT25 directly interacts with the BBSome or if IFT25 regulates the entire IFTparticle/motor/BBSome assembly. Pull-down experiments using IFT25 could provide evidence for the direct interaction of IFT25 and BBSome components. If a direct linkage is discovered, it would be interesting to see if the nucleotide status of IFT27 plays a role in the interaction.

REFERENCES


1 Ishikawa, H. & Marshall, W. F. Ciliogenesis: building the cell's antenna. *Nature Reviews. Molecular Cell Biology* **12**, 222-234, (2011).

2 Pazour, G. J. & Witman, G. B. The vertebrate primary cilium is a sensory organelle. *Current Opinion in Cell Biology* **15**, 105-110 (2003).

3 Kozminski, K. G., Johnson, K. A., Forscher, P. & Rosenbaum, J. L. A motility in the eukaryotic flagellum unrelated to flagellar beating. *Proceedings of the National Academy of Sciences of the United States of America* **90**, 5519-5523 (1993).

4 Rosenbaum, J. Intraflagellar transport. *Current Biology* **12**, R125, (2002).

5 Cole, D. G. Diener, D.R., Himelblau, A.L., Beech, P.L., Fuster, J.C., & Rosenbaum, J.L. *Chlamydomonas* kinesin-II-dependent intraflagellar transport (IFT): IFT particles contain proteins required for ciliary assembly in *Caenorhabditis elegans* sensory neurons. *The Journal of Cell Biology* **141**, 993-1008 (1998).

6 Kozminski, K. G., Beech, P. L. & Rosenbaum, J. L. The *Chlamydomonas* kinesin-like protein FLA10 is involved in motility associated with the flagellar membrane. *The Journal of Cell Biology* **131**, 1517-1527 (1995).

7 Pazour, G. J., Wilkerson, C. G. & Witman, G. B. A dynein light chain is essential for the retrograde particle movement of intraflagellar transport (IFT). *The Journal of Cell Biology* **141**, 979-992 (1998).

8 Pazour, G. J., Dickert, B. L. & Witman, G. B. The DHC1b (DHC2) isoform of cytoplasmic dynein is required for flagellar assembly. *The Journal of Cell Biology* **144**, 473-481 (1999).

9 Rompolas, P., Pedersen, L. B., Patel-King, R. S. & King, S. M. *Chlamydomonas* FAP133 is a dynein intermediate chain associated with the retrograde intraflagellar transport motor. *Journal of Cell Science* **120**, 3653-3665, (2007).

10 Asai, D. J., Rajagopalan, V. & Wilkes, D. E. Dynein-2 and ciliogenesis in *Tetrahymena*. *Cell Motility and the Cytoskeleton* **66**, 673-677, (2009).

11 Hao, L., Efimenko, E., Swoboda, P. & Scholey, J. M. The retrograde IFT machinery of *C. elegans* cilia: two IFT dynein complexes? *PloS ONE* **6**, e20995, (2011).

12 Scholey, J. M. Intraflagellar transport motors in cilia: moving along the cell's antenna. *The Journal of Cell Biology* **180**, 23-29, (2008).

13 Scholey, J. M. Intraflagellar transport. *Annual Review of Cell and Developmental Biology* **19**, 423-443, (2003).

14 Porter, M. E., Bower, R., Knott, J. A., Byrd, P. & Dentler, W. Cytoplasmic dynein heavy chain 1b is required for flagellar assembly in *Chlamydomonas. Molecular Biology of the Cell* **10**, 693-712 (1999).

15 Pigino, G. Geimer, S., Lanzavecchia, S., Paccagnini, E. Canetele, F., Diener, D.R., Rosenbaum, & J.L. Lupetti, P. Electron-tomographic analysis of intraflagellar transport particle trains in situ. *The Journal of Cell Biology* **187**, 135-148, (2009).

16 Marshall, W. F. & Rosenbaum, J. L. Intraflagellar transport balances continuous turnover of outer doublet microtubules: implications for flagellar length control. *The Journal of Cell Biology* **155**, 405-414, (2001).

17 Nachury M.V., Loktev A.V., Zhang Q., Westlake C.J., Peränen J., Merdes A., Slusarski D.C., Scheller R.H., Bazan J.F., Sheffield V.C., & Jackson P.K... A core complex of BBS proteins cooperates with the GTPase Rab8 to promote ciliary membrane biogenesis. *Cell* **129**, 1201-1213 (2007).

18 Lechtreck, K. F. Johnson E.C., Sakai T., Cochran D., Ballif B.A., Rush J., Pazour G.J., Ikebe M., & Witman G.B.. The *Chlamydomonas reinhardtii* BBSome is an IFT cargo required for export of specific signaling proteins from flagella. *The Journal of Cell Biology* **187**, 1117-1132, (2009).

19 Cole, D. G. Chinn S.W., Wedaman K.P., Hall K., Vuong T., & Scholey J.M.. Novel heterotrimeric kinesin-related protein purified from sea urchin eggs. *Nature* **366**, 268-270, (1993).

20 Cole, D. G. The intraflagellar transport machinery of *Chlamydomonas reinhardtii*. *Traffic* **4**, 435-442 (2003).

21 Matsuura, K., Lefebvre, P. A., Kamiya, R. & Hirono, M. Kinesin-II is not essential for mitosis and cell growth in *Chlamydomonas*. *Cell Motility and the Cytoskeleton* **52**, 195-201, (2002).

22 Signor, D. Wedaman K.P., Orozco J.T., Dwyer N.D., Bargmann C.I., Rose L.S., & Scholey J.M. Role of a class DHC1b dynein in retrograde transport of IFT motors and IFT raft particles along cilia, but not dendrites, in chemosensory neurons of living *Caenorhabditis elegans*. *The Journal of Cell Biology* **147**, 519-530 (1999).

23 Snow, J. J. Ou G., Gunnarson A.L., Walker M.R., Zhou H.M., Brust-Mascher I., & Scholey J.M. Two anterograde intraflagellar transport motors cooperate to build sensory cilia on *C. elegans* neurons. *Nature Cell Biology* **6**, 1109-1113 (2004).

24 Morsci, N. S. & Barr, M. M. Kinesin-3 KLP-6 regulates intraflagellar transport in male-specific cilia of *Caenorhabditis elegans*. *Current Biology* **21**, 1239-1244, (2011).

25 Mueller, J., Perrone, C. A., Bower, R., Cole, D. G. & Porter, M. E. The FLA3 KAP subunit is required for localization of kinesin-2 to the site of flagellar assembly and processive anterograde intraflagellar transport. *Molecular Biology of the Cell* **16**, 1341-1354 (2005).

26 Li, C. Inglis P.N., Leitch C.C., Efimenko E., Zaghloul N.A., Mok C.A., Davis E.E., Bialas N.J., Healey M.P., Héon E., Zhen M., Swoboda P., Katsanis N., & Leroux M.R. An essential role for DYF-11/MIP-T3 in assembling functional intraflagellar transport complexes. *PLoS Genetics* **4**, e1000044, (2008).

27 Dishinger, J. F. Kee, H.L., Jenkins, P.M., Fan, S., Hurd, T.W., Hammond, J.W., Truong, Y.N., Margolis, B., Martens, J.R., & Verhey, K.J.. Ciliary entry of the kinesin-2 motor KIF17 is regulated by importin-beta2 and RanGTP. *Nature Cell Biology* **12**, 703-710, (2010).

28 Hou, Y., Pazour, G. J. & Witman, G. B. A dynein light intermediate chain, D1bLIC, is required for retrograde intraflagellar transport. *Molecular Biology of the Cell* **15**, 4382-4394, (2004).

29 Perrone, C. A. Tritschler D., Taulman P., Bower R., Yoder B.K., Porter M.E. A novel dynein light intermediate chain colocalizes with the retrograde motor for intraflagellar transport at sites of axoneme assembly in *Chlamydomonas* and mammalian cells. *Molecular Biology of the Cell* **14**, 2041-2056 (2003).

30 Schafer, J. C., Haycraft, C. J., Thomas, J. H., Yoder, B. K. & Swoboda, P. XBX-1 encodes a dynein light intermediate chain required for retrograde intraflagellar transport and cilia assembly in *Caenorhabditis elegans*. *Molecular Biology of the Cell* **14**, 2057-2070, (2003).

31 Pedersen, L. B. & Rosenbaum, J. L. Intraflagellar transport (IFT) role in ciliary assembly, resorption and signalling. *Current Topics in Developmental Biology* **85**, 23-61, (2008).

32 Piperno, G. Siuda E., Henderson S., Segil M., Vaananen H., Sassaroli M. Distinct mutants of retrograde intraflagellar transport (IFT) share similar morphological and molecular defects. *The Journal of Cell Biology* **143**, 1591-1601 (1998).

33 Iomini, C., Li, L., Esparza, J. M. & Dutcher, S. K. Retrograde intraflagellar transport mutants identify complex A proteins with multiple genetic interactions in *Chlamydomonas reinhardtii*. *Genetics* **183**, 885-896, (2009).

34 Williamson, S. M., Silva, D. A., Richey, E. & Qin, H. Probing the role of IFT particle complex A and B in flagellar entry and exit of IFT-dynein in *Chlamydomonas*. *Protoplasma* **249**, 851-856, (2012).

35 Lucker, B. F. Behal R.H., Qin H., Siron L.C., Taggart W.D., Rosenbaum J.L., Cole D.G. Characterization of the intraflagellar transport complex B core: direct interaction of the IFT81 and IFT74/72 subunits. *The Journal of Biological Chemistry* **280**, 27688-27696, (2005).

36 Lucker, B. F., Miller, M. S., Dziedzic, S. A., Blackmarr, P. T. & Cole, D. G. Direct interactions of intraflagellar transport complex B proteins IFT88, IFT52, and IFT46. *The Journal of Biological Chemistry* **285**, 21508-21518, (2010).

37 Taschner, M., Bhogaraju, S., Vetter, M., Morawetz, M. & Lorentzen, E. Biochemical mapping of interactions within the intraflagellar transport (IFT) B core complex: IFT52 binds directly to four other IFT-B subunits. *The Journal of Biological Chemistry* **286**, 26344-26352, (2011).

38 Behal, R. H. Miller M.S., Qin H., Lucker B.F., Jones A., Cole D.G. Subunit interactions and organization of the *Chlamydomonas reinhardtii* intraflagellar transport complex A proteins. *The Journal of Biological Chemistry* **287**, 11689-11703, (2012).

39 Qin, J., Lin, Y., Norman, R. X., Ko, H. W. & Eggenschwiler, J. T. Intraflagellar transport protein 122 antagonizes Sonic Hedgehog signaling and controls ciliary localization of pathway components. *Proceedings of the National Academy of Sciences of the United States of America* **108**, 1456-1461, (2011).

40 Lee, E., Sivan-Loukianova, E., Eberl, D. F. & Kernan, M. J. An IFT-A protein is required to delimit functionally distinct zones in mechanosensory cilia. *Current Biology* **18**, 1899-1906, (2008).

41 Pedersen, L. B., Geimer, S. & Rosenbaum, J. L. Dissecting the molecular mechanisms of intraflagellar transport in *Chlamydomonas*. *Current Biology* **16**, 450-459, (2006).

42 Ou, G., Blacque, O. E., Snow, J. J., Leroux, M. R. & Scholey, J. M. Functional coordination of intraflagellar transport motors. *Nature* **436**, 583-587 (2005).

43 Hou, Y. Qin H., Follit J.A., Pazour G.J., Rosenbaum J.L., & Witman G.B. Functional analysis of an individual IFT protein: IFT46 is required for transport of outer dynein arms into flagella. *The Journal of Cell Biology* **176**, 653-665, (2007).

44 Ahmed, N. T., Gao, C., Lucker, B. F., Cole, D. G. & Mitchell, D. R. ODA16 aids axonemal outer row dynein assembly through an interaction with the intraflagellar transport machinery. *The Journal of Cell Biology* **183**, 313-322, (2008).

45 Pazour, G. J. Dickert B.L., Vucica Y., Seeley E.S., Rosenbaum J.L., Witman G.B., & Cole D.G. *Chlamydomonas* IFT88 and its mouse homologue, polycystic kidney disease gene tg737, are required for assembly of cilia and flagella. *The Journal of Cell Biology* **151**, 709-718 (2000).

46 Richey, E. A. & Qin, H. Dissecting the sequential assembly and localization of intraflagellar transport particle complex B in *Chlamydomonas*. *PloS ONE* **7**, e43118, (2012).

47 Krock, B. L. & Perkins, B. D. The intraflagellar transport protein IFT57 is required for cilia maintenance and regulates IFT-particle-kinesin-II dissociation in vertebrate photoreceptors. *Journal of Cell Science* **121**, 1907-1915 (2008).

48 Follit, J. A., Tuft, R. A., Fogarty, K. E. & Pazour, G. J. The intraflagellar transport protein IFT20 is associated with the Golgi complex and is required for cilia assembly. *Molecular Biology of the Cell* **17**, 3781-3792 (2006).

49 Rosenbaum, J. L. & Witman, G. B. Intraflagellar transport. *Nature Reviews. Molecular Cell Biology* **3**, 813-825, (2002).

50 Craige, B., Tsao C.C., Diener D.R., Hou Y., Lechtreck K.F., Rosenbaum J.L., & Witman G.B. CEP290 tethers flagellar transition zone microtubules to the membrane and regulates flagellar protein content. *The Journal of Cell Biology* **190**, 927-940, (2010).

51 Omran, H. NPHP proteins: gatekeepers of the ciliary compartment. *The Journal of Cell Biology* **190**, 715-717, (2010).

52 Williams, C. L., Li C., Kida K., Inglis P.N., Mohan S., Semenec L., Bialas N.J., Stupay R.M., Chen N., Blacque O.E., Yoder B.K., & Leroux M.R. MKS and NPHP modules cooperate to establish basal body/transition zone membrane associations and ciliary gate function during ciliogenesis. *The Journal of Cell Biology* **192**, 1023-1041, (2011).

53 Nachury, M. V., Seeley, E. S. & Jin, H. Trafficking to the ciliary membrane: how to get across the periciliary diffusion barrier? *Annual Review of Cell and Developmental Biology* **26**, 59-87, (2010).

54 Francis, S. S., Sfakianos, J., Lo, B. & Mellman, I. A hierarchy of signals regulates entry of membrane proteins into the ciliary membrane domain in epithelial cells. *The Journal of Cell Biology* **193**, 219-233, (2011).

55 Takeda, T., McQuistan, T., Orlando, R. A. & Farquhar, M. G. Loss of glomerular foot processes is associated with uncoupling of podocalyxin from the actin cytoskeleton. *Journal of Clinical Investigation* **108**, 289-301, (2001).

56 Cevik, S., Hori Y., Kaplan O.I., Kida K., Toivenon T., Foley-Fisher C., Cottell D., Katada T., Kontani K., Blacque O.E.. Joubert syndrome Arl13b functions at ciliary membranes and stabilizes protein transport in *Caenorhabditis elegans*. *The Journal of Cell Biology* **188**, 953-969, (2010).

57 Li, Y., Wei, Q., Zhang, Y., Ling, K. & Hu, J. The small GTPases ARL-13 and ARL-3 coordinate intraflagellar transport and ciliogenesis. *The Journal of Cell Biology* **189**, 1039-1051, (2010).

58 Duldulao, N. A., Lee, S. & Sun, Z. Cilia localization is essential for in vivo functions of the Joubert syndrome protein Arl13b/Scorpion. *Development* **136**, 4033-4042, (2009).

59 Westlake, C. J., Baye L.M., Nachury M.V., Wright K.J., Ervin K.E., Phu L., Chalouni C., Beck J.S., Kirkpatrick D.S., Slusarski D.C., Sheffield V.C., Scheller R.H., & Jackson P.K. Primary cilia membrane assembly is initiated by Rab11 and transport protein particle II (TRAPPII) complex-dependent trafficking of Rabin8 to the centrosome. *Proceedings of the National Academy of Sciences of the United States of America* **108**, 2759-2764, (2011).

60 Knodler, A. , Feng S., Zhang J., Zhang X., Das A., Peränen J., & Guo W. Coordination of Rab8 and Rab11 in primary ciliogenesis. *Proceedings of the National Academy of Sciences of the United States of America* **107**, 6346-6351, (2010).

61 Mazelova, J. Astuto-Gribble L., Inoue H., Tam B.M., Schonteich E., Prekeris R., Moritz O.L., Randazzo P.A., & Deretic D. Ciliary targeting motif VxPx directs assembly of a trafficking module through Arf4. *The EMBO Journal* **28**, 183-192, (2009).

62 Ward, H. H., Brown-Glaberman U., Wang J., Morita Y., Alper S.L., Bedrick E.J., Gattone V.H. 2nd, Deretic D., & Wandinger-Ness A. A conserved signal and GTPase complex are required for the ciliary transport of polycystin-1. *Molecular Biology of the Cell* **22**: 3289–3305 (2011).

63 Boehlke, C., Bashkurov M., Buescher A., Krick T., John A.K., Nitschke R., Walz G., & Kuehn E.W. Differential role of Rab proteins in ciliary trafficking: Rab23 regulates smoothened levels. *Journal of Cell Science* **123**, 1460-1467, (2010).

64 Wang, Z., Fan, Z. C., Williamson, S. M. & Qin, H. Intraflagellar transport (IFT) protein IFT25 is a phosphoprotein component of IFT complex B and physically interacts with IFT27 in Chlamydomonas. *PloS ONE* **4**, e5384, (2009).

65 Qin, H., Wang, Z., Diener, D. & Rosenbaum, J. Intraflagellar transport protein 27 is a small G protein involved in cell-cycle control. *Current Biology* **17**, 193-202, (2007).

66 Bhogaraju, S., Taschner, M., Morawetz, M., Basquin, C. & Lorentzen, E. Crystal structure of the intraflagellar transport complex 25/27. *The EMBO Journal* **30**, 1907-1918, (2011).

67 Ou, G., Koga M., Blacque O.E., Murayama T., Ohshima Y., Schafer J.C., Li C., Yoder B.K., Leroux M.R., & Scholey JM.. Sensory ciliogenesis in *Caenorhabditis elegans*: assignment of IFT components into distinct modules based on transport and phenotypic profiles. *Molecular Biology of the Cell* **18**, 1554-1569, (2007).

68 Schafer, J. C., Winkelbauer M.E., Williams C.L., Haycraft C.J., Desmond R.A., & Yoder B.K.. IFTA-2 is a conserved cilia protein involved in pathways regulating longevity and dauer formation in *Caenorhabditis elegans*. *Journal of Cell Science* **119**, 4088-4100, (2006).

69 Adhiambo, C., Blisnick, T., Toutirais, G., Delannoy, E. & Bastin, P. A novel function for the atypical small G protein Rab-like 5 in the assembly of the trypanosome flagellum. *Journal of Cell Science* **122**, 834-841, (2009).

70 Iomini, C., Babaev-Khaimov, V., Sassaroli, M. & Piperno, G. Protein particles in *Chlamydomonas* flagella undergo a transport cycle consisting of four phases. *The Journal of Cell Biology* **153**, 13-24 (2001).

71 Tam, L. W., Wilson, N. F. & Lefebvre, P. A. A CDK-related kinase regulates the length and assembly of flagella in *Chlamydomonas*. *The Journal of Cell Biology* **176**, 819-829, (2007).

72 Huang, B., Rifkin, M. R. & Luck, D. J. Temperature-sensitive mutations affecting flagellar assembly and function in *Chlamydomonas reinhardtii*. *The Journal of Cell Biology* **72**, 67-85 (1977).

73 Adams, G. M., Huang, B. & Luck, D. J. Temperature-Sensitive, Assembly-Defective Flagella Mutants of *Chlamydomonas reinhardtii*. *Genetics* **100**, 579-586 (1982).

74 Walther, Z., Vashishtha, M. & Hall, J. L. The *Chlamydomonas* FLA10 gene encodes a novel kinesin-homologous protein. *The Journal of Cell Biology* **126**, 175-188 (1994).

75 Silva, D. A., Huang, X., Behal, R. H., Cole, D. G. & Qin, H. The RABL5 homolog IFT22 regulates the cellular pool size and the amount of IFT particles partitioned to the flagellar compartment in *Chlamydomonas reinhardtii*. *Cytoskeleton* **69**, 33-48, (2012).

76 Brazelton, W. J., Amundsen, C. D., Silflow, C. D. & Lefebvre, P. A. The bld1 mutation identifies the *Chlamydomonas* osm-6 homolog as a gene required for flagellar assembly. *Current Biology* **11**, 1591-1594 (2001).

77 Mukhopadhyay, S., Wen X., Chih B., Nelson C.D., Lane W.S., Scales S.J., & Jackson P.K. TULP3 bridges the IFT-A complex and membrane phosphoinositides to promote trafficking of G protein-coupled receptors into primary cilia. *Genes & Development* **24**, 2180-2193, (2010).

78 Deane, J. A., Cole, D. G., Seeley, E. S., Diener, D. R. & Rosenbaum, J. L. Localization of intraflagellar transport protein IFT52 identifies basal body transitional fibers as the docking site for IFT particles. *Current Biology* **11**, 1586-1590 (2001).

79 Cole, D. G. & Snell, W. J. SnapShot: Intraflagellar transport. *Cell* **137**, 784-784 e781, (2009).

80 Garcia-Gonzalo, F. R., Corbit, K.C., Sirerol-Piquer, M.S., Ramaswami, G., Otto, E.A., Noriega, T.R., Seol, A.D., Robinson, J.F., Bennett, C.L., Josifova, D.J., García-Verdugo, J.M., Katsanis, N., Hildebrandt, F., & Reiter, J.F. A transition zone complex regulates mammalian ciliogenesis and ciliary membrane composition. *Nature Genetics* **43**, 776-784, (2011).

81 Sonenberg, N. & Dever, T. E. Eukaryotic translation initiation factors and regulators. *Current Opinion in Structural Biology* **13**, 56-63 (2003).

82 Bartel, D. P. MicroRNAs: genomics, biogenesis, mechanism, and function. *Cell* **116**, 281-297 (2004).

83 Bartel, D. P. & Chen, C. Z. Micromanagers of gene expression: the potentially widespread influence of metazoan microRNAs. *Nature Reviews. Genetics* **5**, 396-400, (2004).

84 Gebauer, F. & Hentze, M. W. Molecular mechanisms of translational control. *Nature Reviews. Molecular Cell Biology* **5**, 827-835, (2004).

85 Keady, B. T., Samtani, R., Tobita, K., Tsuchya, M., San Agustin, J.T., Follit, J.A., Jonassen, J.A., Subramanian, R., Lo, C.W., & Pazour, G.J. IFT25 links the signal-dependent movement of Hedgehog components to intraflagellar transport. *Development Cell* **22**, 940-951, (2012).

86 Jin, H., White, S.R., Shida, T., Schulz, S., Aguiar, M., Gygi, S.P., Bazan, J.F., & Nachury, M.V. The conserved Bardet-Biedl syndrome proteins assemble a coat that traffics membrane proteins to cilia. *Cell* **141**, 1208-1219, (2010).

87 Wei, Q., Zhang, Y., Li, Y., Zhang, Q., Ling K., & Hu, J. The BBSome controls IFT assembly and turnaround in cilia. *Nature Cell Biology* **14**, 950-957, (2012).

88 Dutcher, S. K., Morrissette, N. S., Preble, A. M., Rackley, C. & Stanga, J. Epsilon-tubulin is an essential component of the centriole. *Molecular Biology of the Cell* **13**, 3859-3869, (2002).

89 Molnar, A., Bassett, A., Thuenemann, E., Schwach, F., Karkare, S., Ossowski, S., Weigel, D., & Baulcombe, D. Highly specific gene silencing by artificial microRNAs in the unicellular alga *Chlamydomonas reinhardtii*. *The Plant Journal for Cell and Molecular Biology* **58**, 165-174, (2009).

90 Qin, H., Diener, D. R., Geimer, S., Cole, D. G. & Rosenbaum, J. L. Intraflagellar transport (IFT) cargo: IFT transports flagellar precursors to the tip and turnover products to the cell body. *The Journal of Cell Biology* **164**, 255-266, (2004).